NATIONAL ADVISORY COMMITTEE FOR AERONAUTICS

TECHNICAL NOTE

No. 1228

JUN 27 1947

TWO-DIMENSIONAL WIND-TUNNEL INVESTIGATION OF A 10.7-PERCENT-THICK SYMMETRICAL TAIL SECTION WITH A 0.40 AIRFOIL-CHORD CONTROL SURFACE AND A 0.20 CONTROL-SURFACE-CHORD TAB

By Albert L. Braslow

Langley Memorial Aeronautical Laboratory
Langley Field, Va.

Washington
June 1947

NACA LIBRARY
LANGLEY MEMORIAL AERONAUTICAL
LABORATORY
Langley Field, Va.

NASA Technical Library
3 1176 01433 3505

NATIONAL ADVISORY COMMITTEE FOR AERONAUTICS

TECHNICAL NOTE NO. 1228

TWO-DIMENSIONAL WIND-TUNNEL INVESTIGATION OF A 10.7-PERCENT-THICK SYMMETRICAL TAIL SECTION WITH A 0.40 AIRFOIL-CHORD CONTROL SURFACE AND A 0.20 CONTROL-SURFACE-CHORD TAB

By Albert L. Braslow

SUMMARY

An investigation was made of a 10.7-percent-thick symmetrical tail section equipped with a flat-side 0.40 airfoil-chord flap having a 0.333 flap-chord overhang and a plain 0.20 flap-chord tab. Airfoil lift, drag, pitching-moment, and flap and tab hinge-moment characteristics were determined at various flap and tab deflections with the control-surface nose gaps sealed and unsealed.

The results of the tests indicated that sealing the tab nose gap generally increased the flap lift effectiveness and the tab hinge-moment effectiveness. Sealing the flap nose gap increased the rate of change of section lift coefficient with both section angle of attack α_o and flap deflection δ_f, negatively increased the rate of change of flap section hinge-moment coefficient c_{h_f} with both α_o and δ_f at a 0° angle of attack and flap deflection, eliminated sharp irregularities in the variation of c_{h_f} with α_o, and greatly reduced all but the minimum values of section drag coefficient at all flap deflections tested. When the flap was deflected beyond the angle at which the flap leading edge unported from the airfoil contour, sudden decreases of lift and large increases of flap and tab hinge moments occurred through a limited range of angle of attack. The effectiveness of the tab in reducing the flap hinge moments was large up to a tab deflection of 10° but decreased appreciably at larger deflections of the tab.

INTRODUCTION

Flight tests of conventional symmetrical tail surfaces made by the Douglas Aircraft Company, Inc., indicated that flat-side elevators and rudders were less subject to air-flow conditions causing undesirable control-surface oscillations than were control surfaces of true-airfoil contour (reference 1). In order to determine other aerodynamic characteristics of a tail section equipped with a flat-side control surface, an investigation was made of a two-dimensional model in the Langley two-dimensional low-turbulence pressure tunnel.

The model was equipped with a 40-percent-airfoil-chord flap designed for use as a rudder or an elevator and having a 20-percent flap-chord tab. The tests included the determination of airfoil section lift, drag, and pitching moments, and flap and tab hinge moments for configurations with the flap and tab nose gaps both sealed and unsealed.

COEFFICIENTS AND SYMBOLS

c_l section lift coefficient (l/qc)

Δc_l increment of c_l due to flap deflection

c_d section drag coefficient (d/qc)

$c_{m_{c/4}}$ section pitching-moment coefficient about quarter-chord point (m/qc^2)

c_{h_f} flap section hinge-moment coefficient (h_f/qc_f^2)

c_{h_t} tab section hinge-moment coefficient (h_t/qc_t^2)

where

l lift per unit span

d drag per unit span

m quarter-chord pitching moment per unit span

h_f flap hinge moment per unit span; positive when trailing edge of flap tends to deflect downward

h_t tab hinge moment per unit span; positive when trailing edge of tab tends to deflect downward

c chord of airfoil with both control surfaces neutral

c_f chord of flap behind flap hinge axis

c_t chord of tab behind tab hinge axis

q free-stream dynamic pressure $\left(\frac{1}{2}\rho V^2\right)$

V free-stream velocity

ρ free-stream density

and

α_o section angle of attack

δ_f flap deflection with respect to airfoil; positive when trailing edge is deflected downward

δ_t tab deflection with respect to flap; positive when trailing edge is deflected downward

c_b chord of overhang balance from flap hinge axis to balance leading edge

R Reynolds number

$$c_{l_\alpha} = \left(\frac{\partial c_l}{\partial \alpha_o}\right)_{\delta_f,\ \delta_t}$$

$$c_{l_{\delta_f}} = \left(\frac{\partial c_l}{\partial \delta_f}\right)_{\alpha_o,\ \delta_t}$$

$$\alpha_{\delta_f} = \left(\frac{\partial \alpha_o}{\partial \delta_f}\right)_{c_l,\ \delta_t}$$

$$c_{h_{f_\alpha}} = \left(\frac{\partial c_{h_f}}{\partial \alpha_o}\right)_{\delta_f,\ \delta_t}$$

$$c_{h_{f_{\delta_f}}} = \left(\frac{\partial c_{h_f}}{\partial \delta_f}\right)_{\alpha_o,\ \delta_t}$$

$$\delta_{f_{\delta_t}} = \left(\frac{\partial \delta_f}{\partial \delta_t}\right)_{c_{h_f},\ \alpha_o} \qquad \text{measured at } \alpha_o = 0^\circ \text{ and } c_{h_f} = 0$$

$$c_{h_{t_\alpha}} = \left(\frac{\partial c_{h_t}}{\partial \alpha_o}\right)_{\delta_f,\ \delta_t}$$

$$c_{h_{t_{\delta_t}}} = \left(\frac{\partial c_{h_t}}{\partial \delta_t}\right)_{\alpha_o,\ \delta_f}$$

$$c_{h_{t_{\delta_f}}} = \left(\frac{\partial c_{h_t}}{\partial \delta_f}\right)_{\alpha_o,\ \delta_t}$$

$$c_{m_{\delta_f}} = \left(\frac{\partial c_{m_{c/4}}}{\partial \delta_f}\right)_{c_l,\ \delta_t} \qquad \text{measured at } c_l = 0,\ \delta_f = 0, \text{ and } \delta_t = 0^\circ$$

$$c_{m_{c_l}} = \left(\frac{\partial c_{m_{c/4}}}{\partial c_l}\right)_{\delta_f,\ \delta_t}$$

The subscripts following the partial derivatives denote the variables held constant when the partial derivatives are taken. The derivatives are obtained at $\alpha_o = 0^\circ$, $\delta_f = 0^\circ$, and $\delta_t = 0^\circ$ except as noted.

MODEL

The profile of the airfoil tested was formed by modifying an NACA 0012 airfoil in such a manner as to provide flat-side control surfaces behind the hinge axes. A sketch and photograph of the model are presented as figures 1 and 2. The modification to the NACA 0012 profile consisted of extending the airfoil chord 12 percent and drawing straight lines from the extended trailing edge tangent to the airfoil surfaces. Extension of the airfoil chord effectively reduced the maximum thickness of the airfoil to 0.107c and moved the position of maximum thickness forward to approximately 0.27c behind the airfoil leading edge. Ordinates for the airfoil are given in table I. The flap of 0.40c had an overhang type of aerodynamic balance of $0.333c_f$ and was equipped with a plain $0.20c_f$ tab. The ordinates for the flap nose shape are given in table II.

The model had a 24-inch chord and was constructed of laminated mahogany with the exception of the tab, which was constructed of dural. The model surfaces were sanded with No. 400 carborundum paper to aerodynamic smoothness. Thin rubber "curtains" and modeling clay were used to seal the flap gap and the tab gap, respectively.

APPARATUS AND TESTS

The model was mounted horizontally in the 3-foot by $7\frac{1}{2}$-foot test section of the Langley two-dimensional low-turbulence pressure tunnel. A manometer arrangement, which integrated the pressures along the floor and ceiling of the tunnel test section, was used to measure lift, and the wake survey method was used to measure drag. Airfoil pitching moments were measured with a torque-tube balance, and control-surface hinge moments were measured with electrical resistance strain gages.

Tests of the model were made at a Reynolds number of 6×10^6 and a Mach number of not greater than 0.11. Airfoil lift, drag, and pitching moments and flap and tab hinge moments were measured through a range of flap and tab deflection. The model was tested with the flap and tab gaps sealed and unsealed in the following combinations: (1) flap gap and tab gap unsealed; (2) flap gap unsealed, tab gap sealed; (3) flap gap sealed, tab gap unsealed. Tab hinge moments were not obtained with the tab gap sealed because of the large friction of a tab seal. Airfoil lift and control-surface hinge moments were

measured at a Reynolds number of 2.5×10^6 as well as 6×10^6 for the neutral position of the flap and tab with both gaps unsealed. The Mach number at Reynolds numbers of 2.5×10^6 and 6×10^6 was essentially the same.

CORRECTIONS AND ACCURACY OF MEASUREMENTS

The following factors were used to correct the tunnel data to free-air conditions:

$$c_l = 0.978c_l'$$

$$c_d = 0.993c_d'$$

$$c_{m_{c/4}} = 0.993c_{m_{c/4}}'$$

$$c_{h_f} = 0.993c_{h_f}'$$

$$c_{h_t} = 0.993c_{h_t}'$$

$$\alpha_o = 1.015\alpha_o'$$

where the primed quantities represent the values measured in the tunnel (reference 2). An additional correction to the moment coefficients due to a distortion of the pressure distribution over the airfoil caused by the tunnel boundaries was not applied inasmuch as the exact shape of the additional loading due to this distortion is not known. Approximate calculations, however, indicate that the additional correction to the values of the moment coefficients are probably in the order of $0.004c_l'$, $0.005c_l'$, and $0.002c_l'$ for the values of $c_{m_{c/4}}$, c_{h_f}, and c_{h_t}, respectively.

From a consideration of the test equipment and the scatter of check runs, the precision of the data is estimated to be as follows:

	At moderate values of c_l and low flap deflections	At values of c_l near stall
α_o	±0.05°	±0.05°
c_l	±.005	±.015
c_d	±.0001	±.0005
$c_{m_{c/4}}$	±.001	±.005
c_{h_f} and c_{h_t}	±.001	±.005

RESULTS AND DISCUSSION

Lift

A summary of the lift parameters c_{l_α}, $c_{l_{\delta_f}}$, and α_{δ_f} is presented in table III for each of the nose gap conditions tested. The basic section lift data for various deflections of the flap and tab and for the control-surface gaps sealed and unsealed are presented in figure 3.

Sealing the tab gap increased the rate of change of section lift coefficient c_l with flap deflection δ_f from 0.066 to 0.070 and had no effect on the rate of change of section lift coefficient with section angle of attack. As a result, the flap effectiveness parameter α_{δ_f} increased from 0.70 to 0.74. With the tab gap open, sealing the flap gap increased $c_{l_{\delta_f}}$ from 0.066 to 0.072 but a corresponding increase in c_{l_α} from 0.095 to 0.104 prevented any appreciable change in the effectiveness parameter. The principal benefit resulting from sealing the flap gap, therefore, is an increase in the control-fixed stability caused by the increase in c_{l_α}.

In order to show the effect on lift effectiveness of flap deflection and flap gap at high flap deflections, the increment of section lift coefficient Δc_l due to flap deflection is plotted against δ_f in figure 4 at section angles of attack of 0°, ±2°,

$\pm 6^{\circ}$, and $\pm 10^{\circ}$. The flap effectiveness decreases as a result of air-flow separation over the flap at section angles of attack greater than approximately 2° when the flap deflection is equal to or greater than 20°, the angle at which the flap leading edge unports. Such a flight condition in which the angle of attack and control-surface deflection may be of like sign might occur, for example, for a vertical tail section during flight with asymmetric power Less serious losses of lift due to unporting of the flap leading edge occur when the section angle of attack is increased in opposition to the flap deflection. This combination of control-surface deflection in opposition to the angle of attack would perhaps occur for an elevator during landing or for a rudder during sideslip.

A comparison of figures 4(a) and 4(b) shows that sealing the flap gap reduces the values of Δc_l at positive section angles of attack throughout the complete range of flap deflection tested. At negative section angles of attack the values of Δc_l were generally greater with the flap sealed than with the flap unsealed except at a flap deflection of 30° in which case the values of Δc_l were greater for the flap unsealed at section angles of attack of -6° and -10°.

A normal scale effect on the lift characteristics of the airfoil with both control surfaces neutral and unsealed results from a change in Reynolds number from 6×10^6 to 2.5×10^6 as shown in figure 5.

Hinge Moments

Flap and tab section hinge-moment coefficients are plotted against airfoil section angle of attack α_o for various deflections of the flap and tab in figures 6 and 7, respectively. Large increases of flap and tab hinge moment occurred through a limited range of angle of attack when the flap was deflected beyond the angle at which the flap leading edge unported from the airfoil contour. A summary of values of important hinge-moment parameters is given in table III.

Sharp irregularities in the variation of c_{h_f} with α_o occurred at a zero flap deflection with the flap gap open (figs. 6(a), 6(b), and 6(e)). Subsequent tuft observations showed that the irregularities were caused by a rapid thickening of the boundary layer over one surface of the flap when a flow of air is induced through the flap gap as the angle of attack is changed. With both control surfaces neutral the asymmetry in the angle of attack at which these irregularities occur is probably caused by the air flow through the flap gap at low angles of attack. Sealing the flap gap eliminates the irregularities in the hinge-moment characteristics as shown in figure 6(g).

Sealing the flap gap or the tab gap negatively increases the values of $c_{h_{f_\alpha}}$, $c_{h_{f_{\delta_f}}}$, $c_{h_{t_\alpha}}$, and $c_{h_{t_{\delta_f}}}$. (See table III and figs. 6 and 7.) The values of $c_{h_{f_\alpha}}$ given in table III for the flap gap unsealed were measured at a section angle of attack of 0° and may be questionable because of the jogs in the hinge-moment curves. The results of previous investigations of conventional airfoils, however, have also indicated a tendency for the values of the hinge-moment parameters c_{h_α} and c_{h_δ} to become more negative as the control-surface gap is decreased (reference 3). The data of figures 6(a) and 6(g) show that at moderate angles of attack, however, the rate of change of c_{h_f} with α_o is less negative for the flap gap sealed than for the flap gap unsealed.

A measure of the effectiveness of the tab in reducing flap hinge moments is the rate of change of flap deflection with the tab deflection required to balance the increment of flap hinge moment caused by the flap deflection at a constant angle of attack. This parameter $\delta_{f_{\delta_t}}$ indicates that the smaller the tab deflection required to balance the increment of c_{h_f} due to a given flap deflection, the greater is the tab hinge-moment effectiveness. Curves of the flap deflection against the tab deflection required to maintain a flap section hinge-moment coefficient of 0 are plotted in figure 8 at angles of attack ranging from -8° to 8° for the flap and tab gaps unsealed. In addition, the variations of δ_f with δ_t through a range of angle of attack from 0° to 8° are plotted for the tab-gap-sealed condition. The curves of figure 8 were obtained by interpolation and extrapolation of the basic flap hinge-moment data presented in figure 6.

The value of $\delta_{f_{\delta_t}}$ at a section angle of attack of 0° for both control-surface gaps unsealed is equal to 1.83 for tab deflections between 0° and -10°. The tab hinge-moment effectiveness at positive flap deflections is greater for negative than for positive angles of attack as shown in figure 8 and is caused by a greater tendency for the air flow to separate over the upper surface of the flap at positive angles of attack. The tab hinge-moment effectiveness decreases appreciably at tab deflections greater than -10° for all angles of attack for which data are available. Sealing the tab gap increases the rate of change of δ_f with δ_t an average of .14 percent at angles of attack from 0° to 8°. The effect of the flap gap on the tab hinge-moment effectiveness was not determined.

The effect of a change in Reynolds number from 6.0×10^6 to 2.5×10^6 on the flap and tab hinge-moment characteristics is shown in figure 9 for both control surfaces neutral and unsealed.

Pitching Moments

Section pitching-moment coefficients are plotted against section lift coefficients in figure 10 for both control gaps unsealed and for the flap gap sealed with the tab gap unsealed. Sealing the flap gap had no appreciable effect on the value of $c_{m_{\delta_f}}$ (table III) or on the value of $c_{m_{c_l}}$ as can be seen from a comparison of figures 10(a) and 10(c).

Drag

Drag characteristics of the airfoil with the control-surface gaps sealed and unsealed are presented in figure 11 for various deflections of the flap and tab. When a flow of air through the flap gap was induced at small angles of attack, a large increase in section drag coefficient occurred (fig. 11(a)). With both control surfaces neutral, the sudden increases in drag were asymmetrical about zero lift but corresponded to the angles of attack at which the irregularities in the flap section hinge-moment coefficients occurred. When the flow of air through the flap gap was eliminated with a seal, the section drag coefficients were symmetrical about zero lift for the neutral position of both control surfaces and a large decrease in all but the minimum values of c_d was obtained at all the flap deflections tested. The value of the minimum section drag coefficient for both control surfaces neutral was 0.0071 for the flap gap unsealed and remained the same for the flap gap sealed. Sealing the tab gap generally decreased the section drag coefficients slightly, although a large increase in drag was still caused by the air flow through the flap gap.

SUMMARY OF RESULTS

The following results were obtained from the two-dimensional wind-tunnel investigation of a 10.7-percent-thick symmetrical tail section equipped with a 0.40c flap having a $0.333c_f$ overhang and a $0.20c_f$ tab.

1. Sealing the tab nose gap generally increased the flap lift effectiveness and tab hinge-moment effectiveness.

2. Sealing the flap gap

   (a) increased the rate of change of section lift coefficient with both section angle of attack α_o and flap deflection δ_f

(b) negatively increased the rate of change of flap section hinge-moment coefficient c_{h_f} with both α_o and δ_f at a 0° angle of attack and flap deflection

(c) eliminated sharp irregularities in the variation of c_{h_f} with α_o

(d) greatly reduced all but the minimum values of section drag coefficient at all flap deflections tested.

3. Sudden decreases of lift and large increases of flap and tab hinge moment occurred through a limited range of angle of attack when the flap was deflected beyond the angle at which the flap leading edge unported from the airfoil contour.

4. The effectiveness of the tab in reducing flap hinge moments was large up to a tab deflection of 10° but decreased appreciably at larger deflections of the tab.

Langley Memorial Aeronautical Laboratory
National Advisory Committee for Aeronautics
Langley Field, Va., December 20, 1946

REFERENCES

1. Root, L. E.: The Effective Use of Aerodynamic Balance on Control Surfaces. Jour. Aero. Sci., vol. 12, no. 2, April 1945, pp. 149-163.

2. Abbott, Ira H., von Doenhoff, Albert E., and Stivers, Louis S., Jr.: Summary of Airfoil Data. NACA ACR No. L5C05, 1945.

3. Purser, Paul E., and Toll, Thomas A.: Analysis of Available Data on Control Surfaces Having Plain-Overhang and Frise Balances. NACA ACR No. L4E13, 1944.

TABLE I

ORDINATES FOR 10.7-PERCENT-THICK TAIL SECTION

[Stations and ordinates given in percent of airfoil chord]

Symmetrical section	
Station	Ordinate
1.116	1.691
2.232	2.335
4.464	3.174
6.700	3.750
8.930	4.181
13.390	4.772
17.860	5.123
22.320	5.304
26.780	5.359
35.710	5.181
44.640	4.726
53.570	4.074
	Straight taper
100.000	0
L.E. radius:	1.410

TABLE II

ORDINATES FOR FLAP NOSE SHAPE

[Stations and ordinates given in percent of movable surface length measured from overhang L.E. to airfoil T.E.]

Symmetrical shape	
Station	Ordinate
1.25	3.64
2.50	4.94
5.00	6.37
7.50	7.13
10.00	7.42
15.00	7.42
20.00	7.04
100.00	0
L.E. radius:	5.3

NATIONAL ADVISORY
COMMITTEE FOR AERONAUTICS

TABLE III

SECTION PARAMETERS MEASURED AT $\alpha_o = 0^\circ$, $\delta_f = 0^\circ$, AND $\delta_t = 0^\circ$

[Except as noted]

Control-surface nose gap	c_{l_α}	$c_{l_{\delta_f}}$	α_{δ_f}	$c_{h_{f_\alpha}}$	$c_{h_{f_{\delta_f}}}$	$\delta_{f_{\delta_t}}$ (1)	$c_{h_{t_\alpha}}$	$c_{h_{t_{\delta_t}}}$	$c_{h_{t_{\delta_f}}}$	$c_{m_{\delta_f}}$ (2)
Flap unsealed Tab unsealed	0.095	0.066	0.70	-0.0030	-0.0043	1.83	-0.0001	-0.0089	-0.0009	-0.0091
Flap unsealed Tab sealed	.095	.070	.74	-.0040	-.0048	2.09	-------	-------	-------	-------
Flap sealed Tab unsealed	.104	.072	.69	-.0045	-.0050	-------	-.0018	-------	-.0019	-.0091

[1] Measured at $\alpha_o = 0^\circ$ and $c_{h_f} = 0$.

[2] Measured at $c_l = 0$, $\delta_f = 0^\circ$, and $\delta_t = 0^\circ$.

NATIONAL ADVISORY COMMITTEE FOR AERONAUTICS

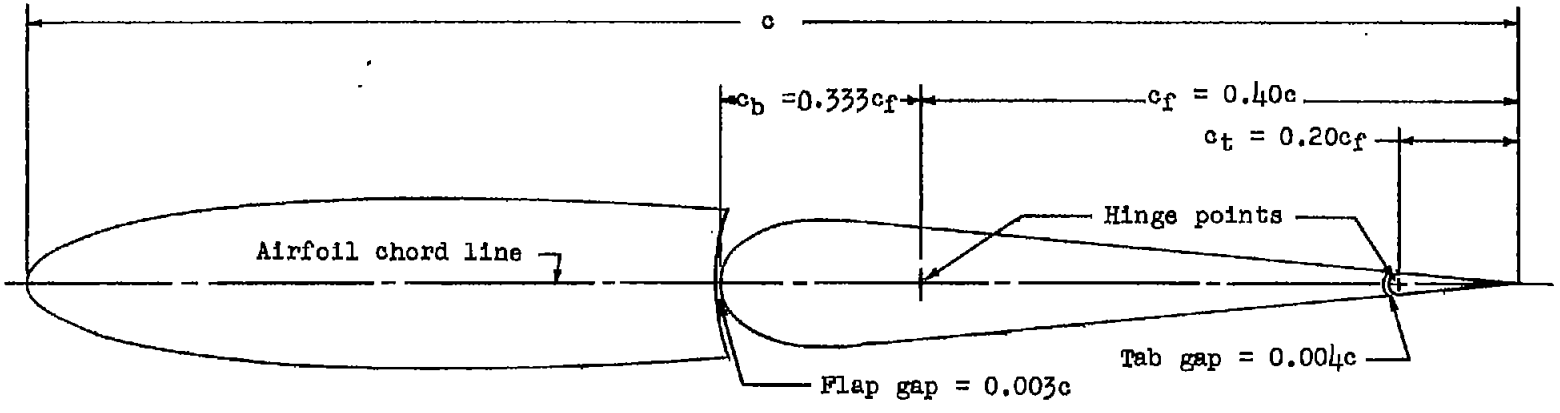

Figure 1.- Sketch of 24-inch-chord 10.7-percent-thick symmetrical tail section.

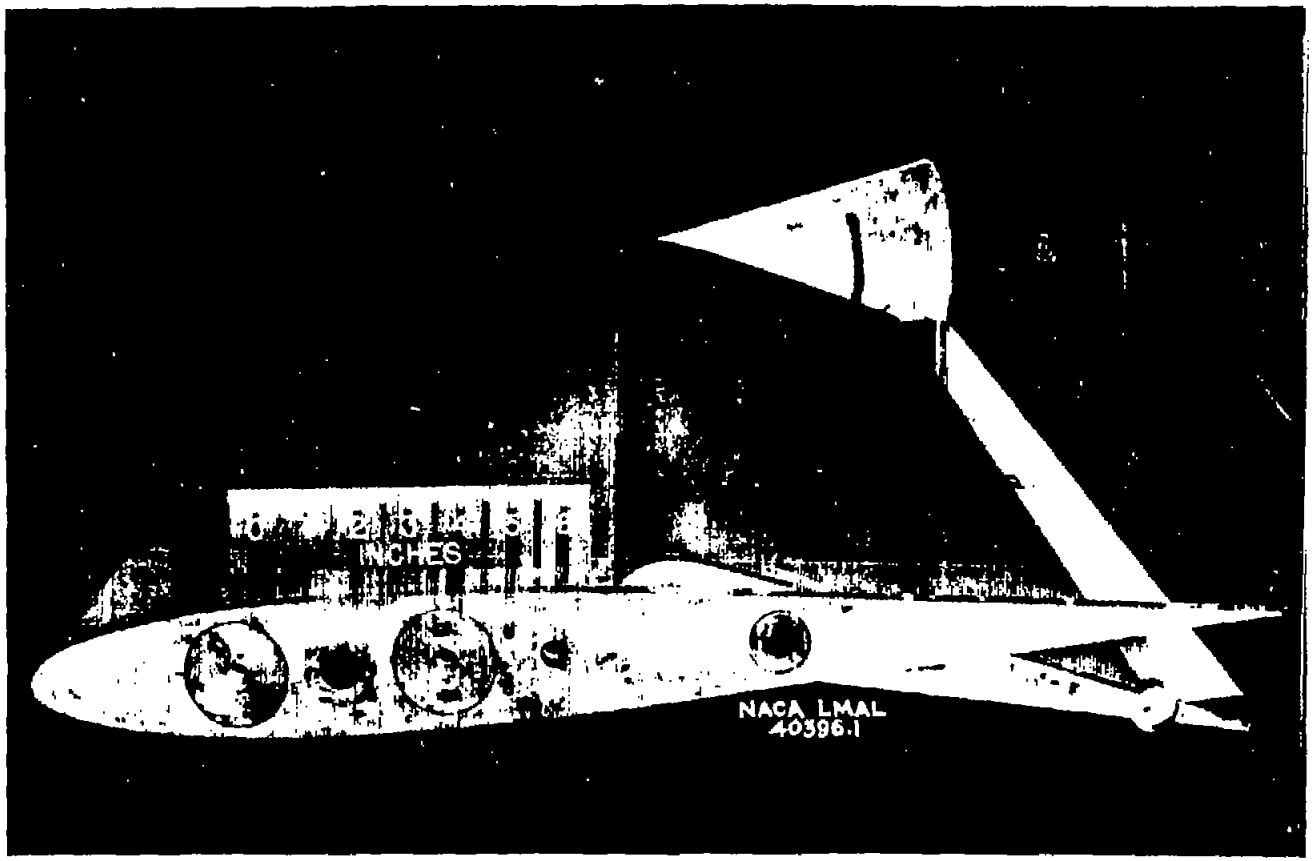

Figure 2.- Photograph of 10.7-percent-thick symmetrical tail section with a 0.40c flap having a 0.333c_f overhang and a 0.20c_f tab. $\delta_f = 20^\circ$, $\delta_t = -20^\circ$.

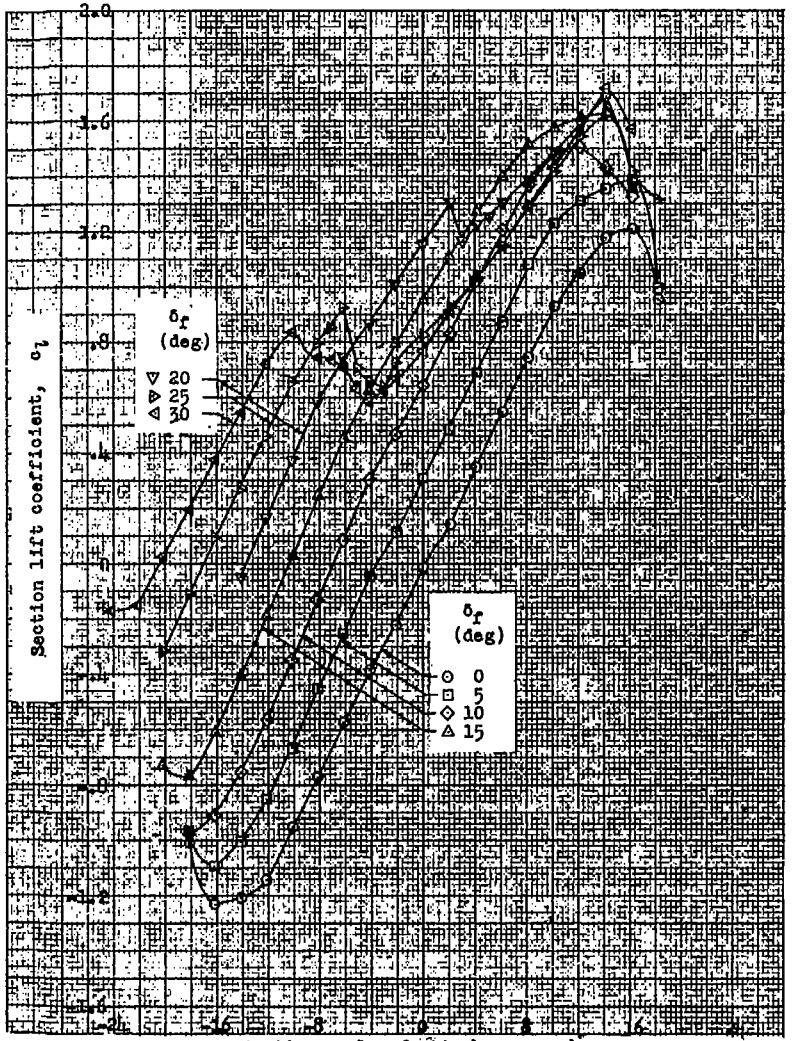

(a) Flap and tab gaps unsealed; $\delta_t = 0^\circ$.

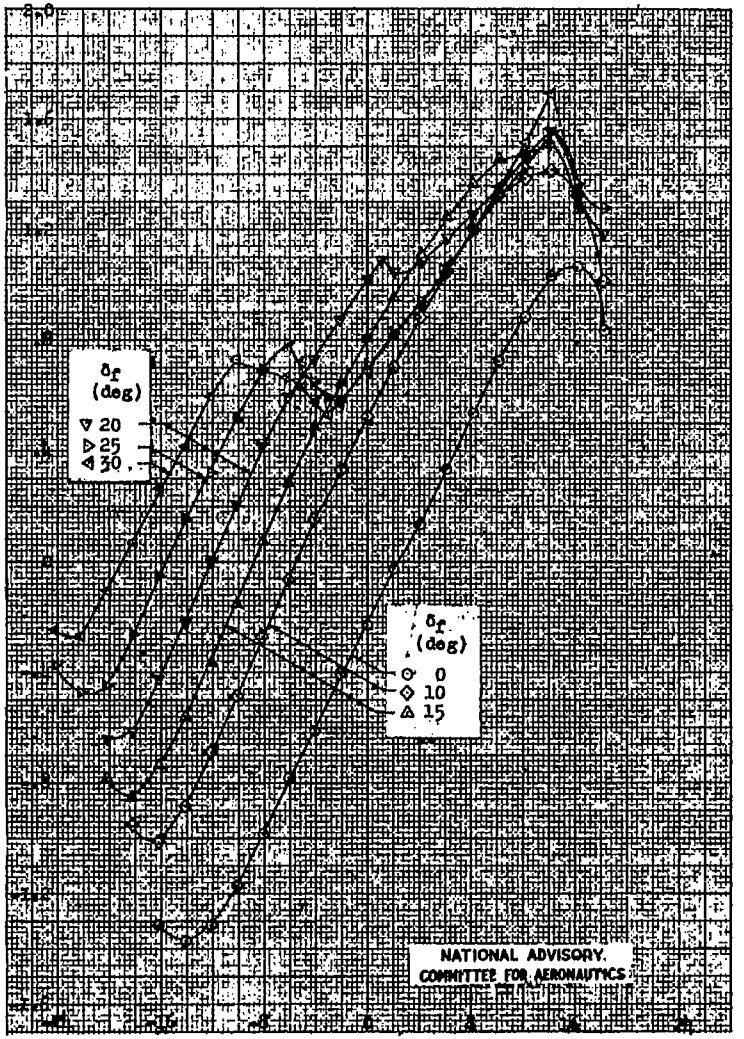

(b) Flap and tab gaps unsealed; $\delta_t = -10^\circ$.

Figure 3.- Lift characteristics of the 10.7-percent-thick symmetrical tail section with a $0.40c$ flap having a $0.333c_f$ overhang and a $0.20c_f$ tab. $R = 6 \times 10^6$ (approx.); tests, TDT 761 and 765.

Fig. 3a,b

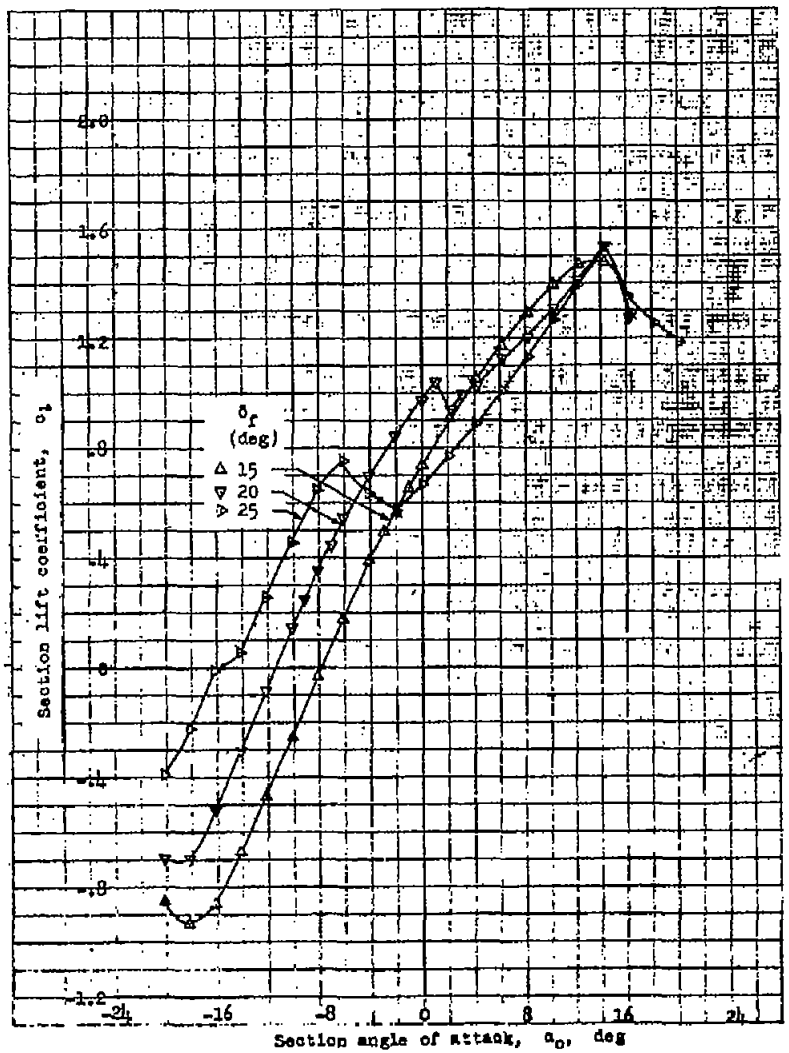

(c) Flap and tab gaps unsealed; $\delta_t = -15^\circ$.

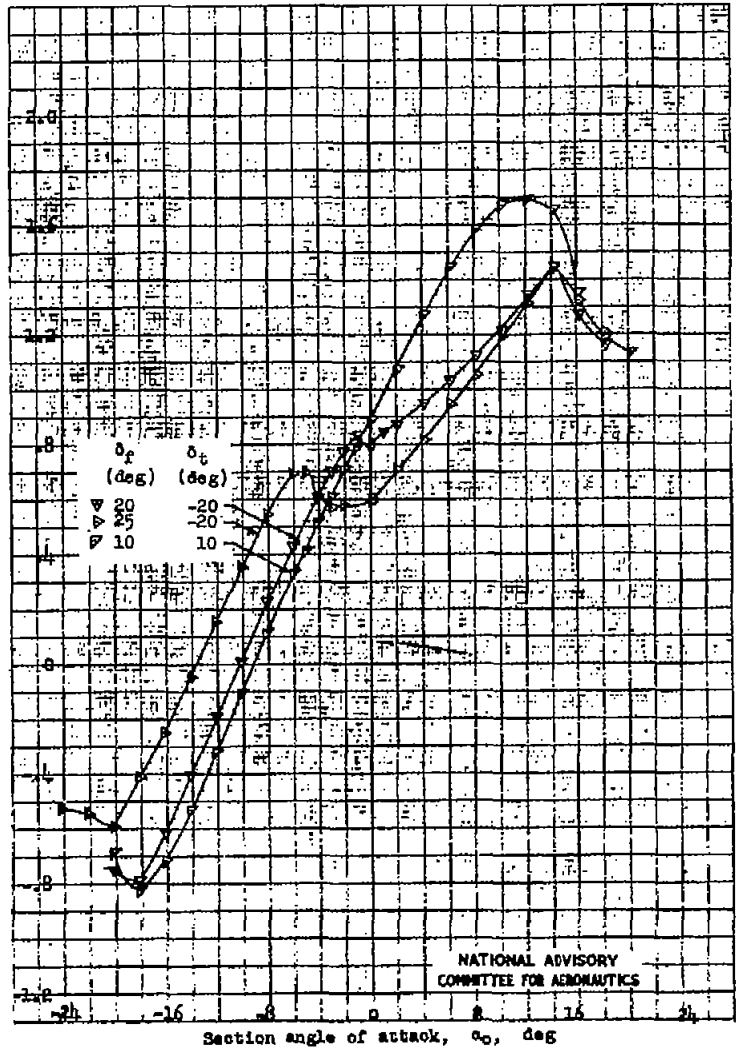

(d) Flap and tab gaps unsealed; $\delta_t = -20^\circ$ and 10°.

Figure 3.- Continued.

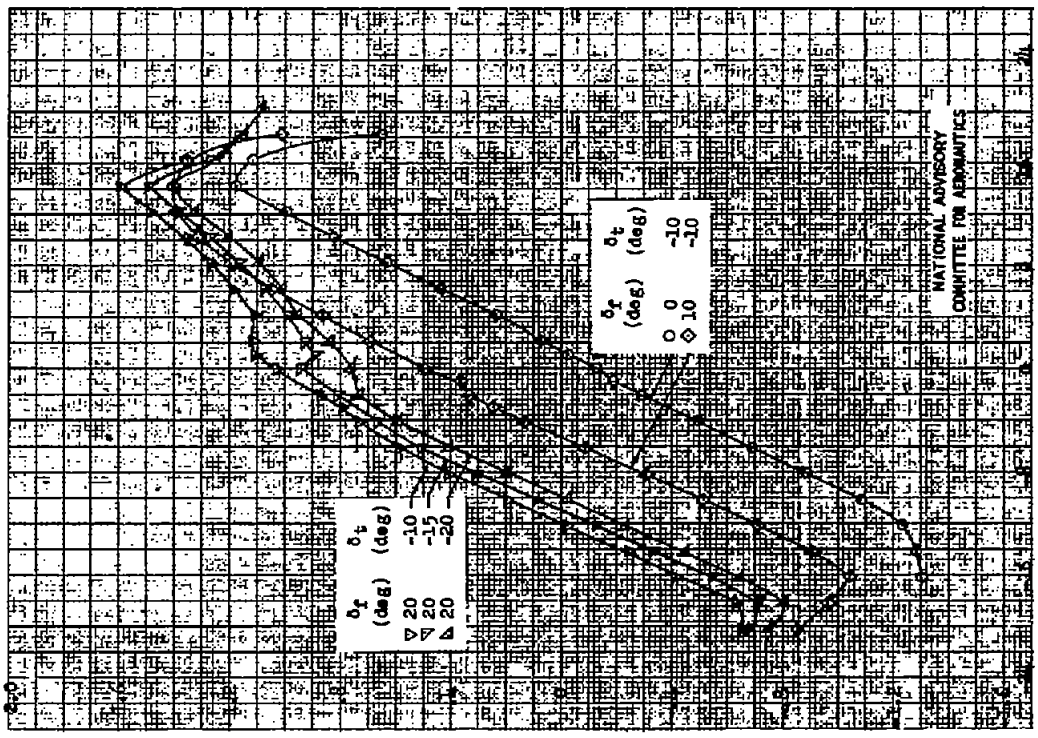

(f) Flap gap unsealed, tab gap sealed; $\delta_t = -10°$, $-15°$, and $-20°$.

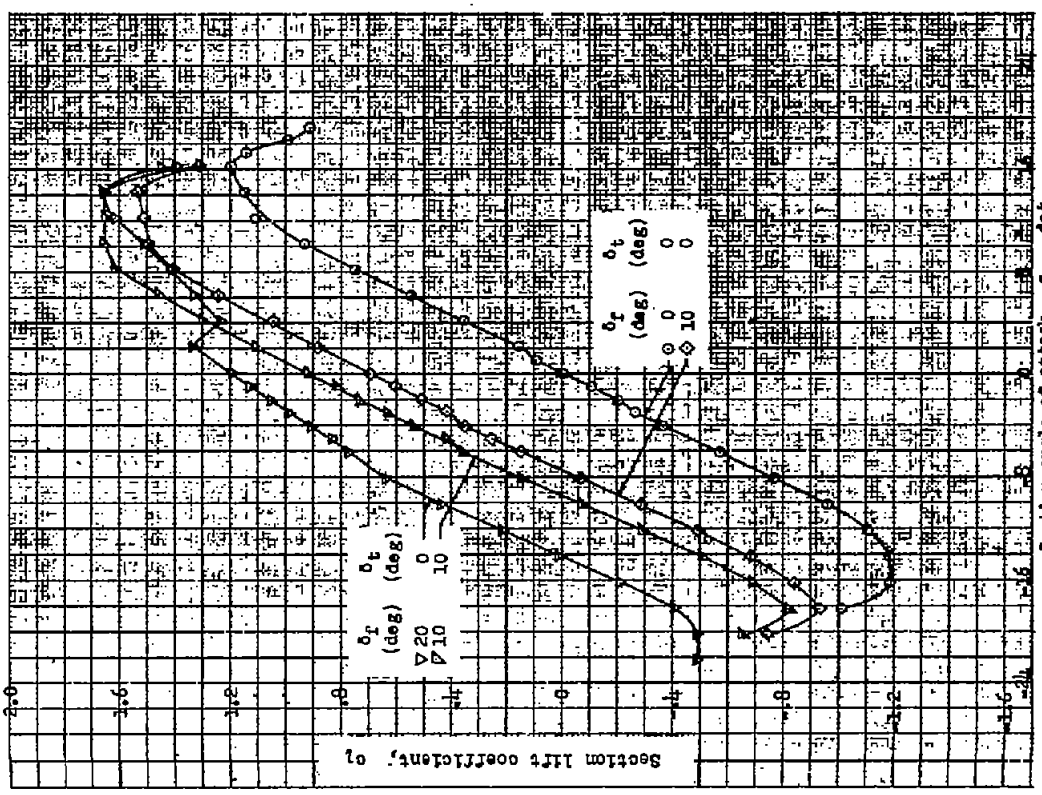

(e) Flap gap unsealed, tab gap sealed; $\delta_t = 0°$ and $10°$.

Figure 3.- Continued.

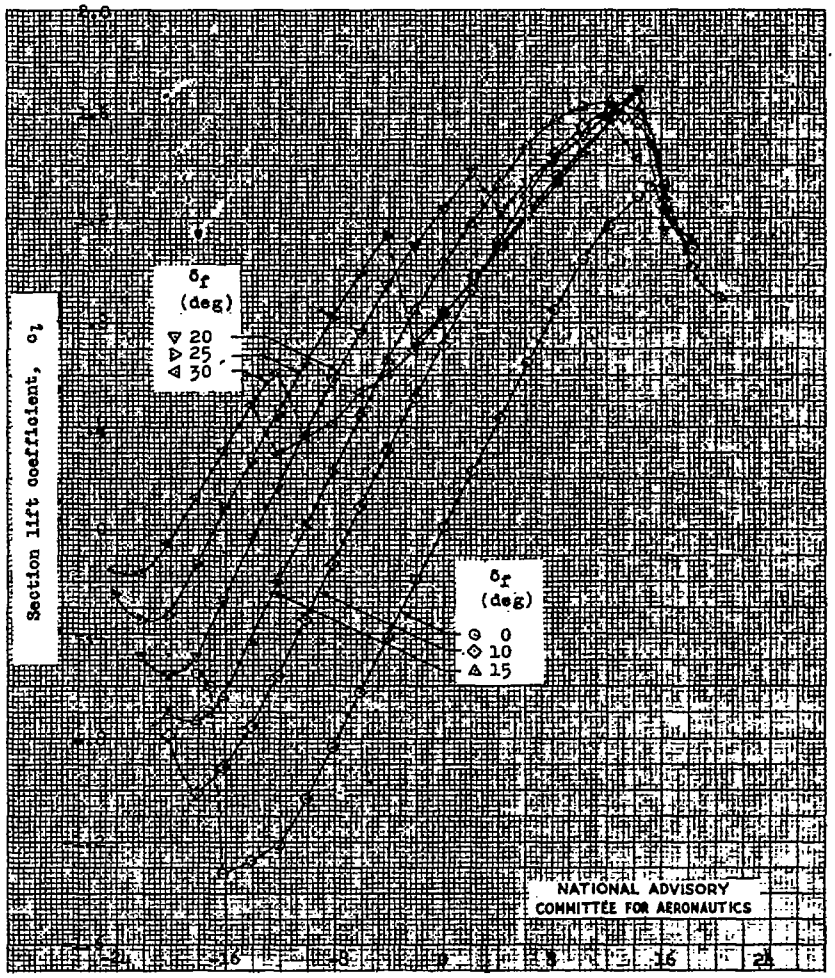

Section angle of attack, α_o, deg

(g) Flap gap sealed, tab gap unsealed; $\delta_t = 0^\circ$.

Figure 3 .- Concluded.

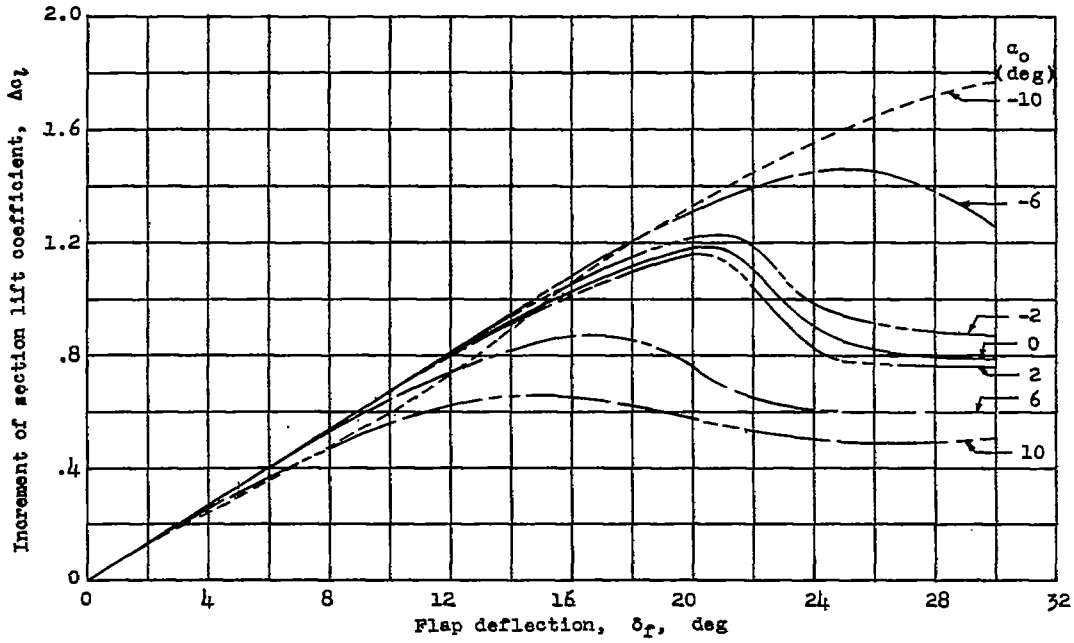

(a) Flap and tab gaps unsealed.

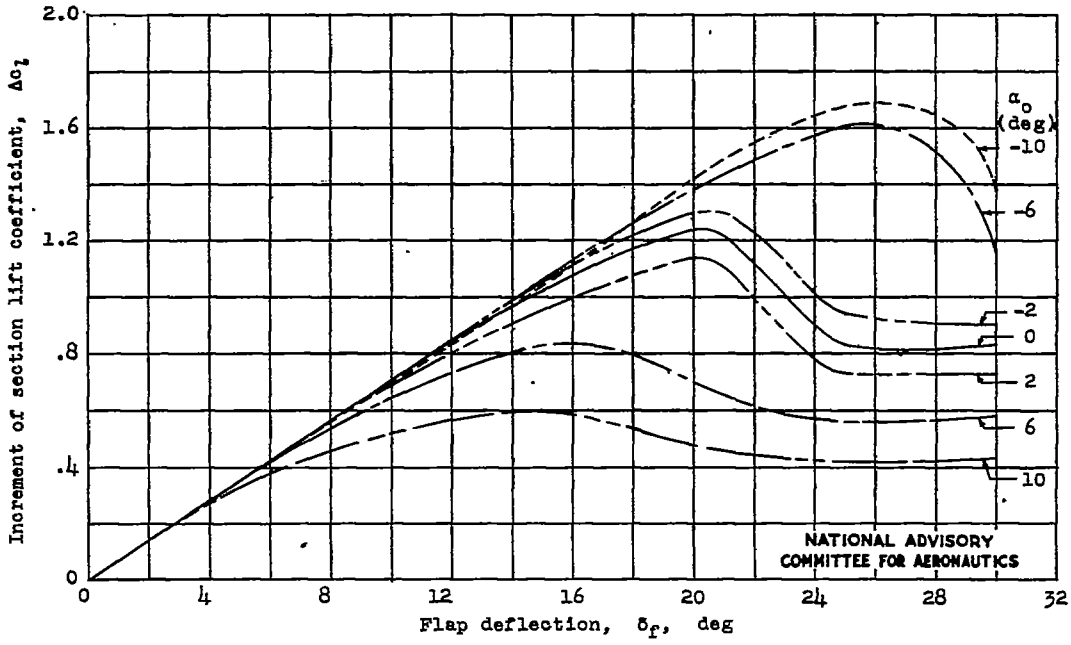

(b) Flap gap sealed, tab gap unsealed.

Figure 4.- Variation of Δc_l with δ_f at constant α_o for the 10.7-percent-thick symmetrical tail section with a 0.40c flap having a 0.333c_f overhang and a 0.20c_f tab. $R = 6 \times 10^6$ (approx.).

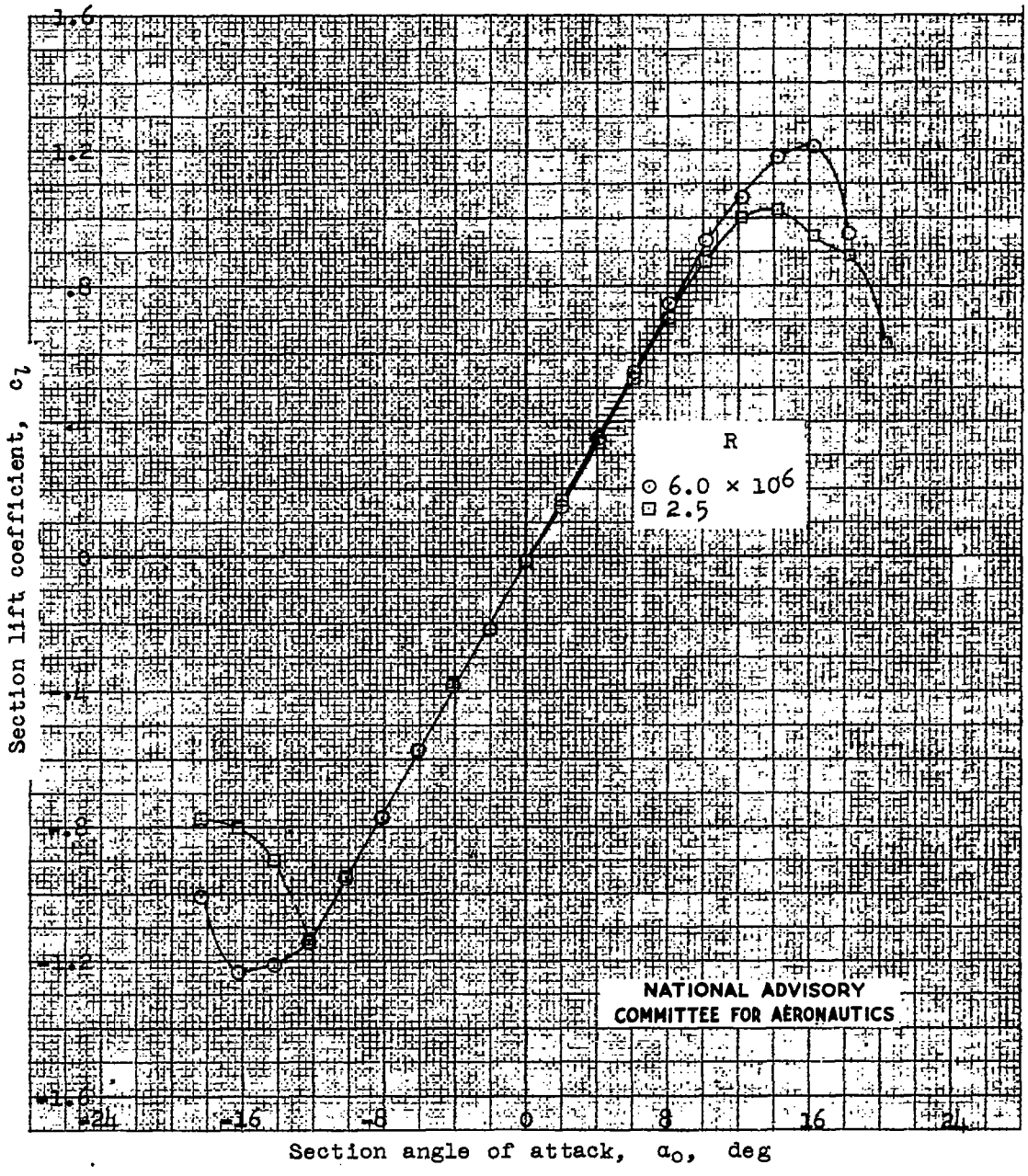

Figure 5.- Scale effect on lift characteristics of the 10.7-percent-thick symmetrical tail section with a 0.40c flap having a $0.333c_f$ overhang and $0.20c_f$ tab. Flap and tab gaps unsealed; $\delta_f = 0^\circ$; $\delta_t = 0^\circ$; test, TDT 761.

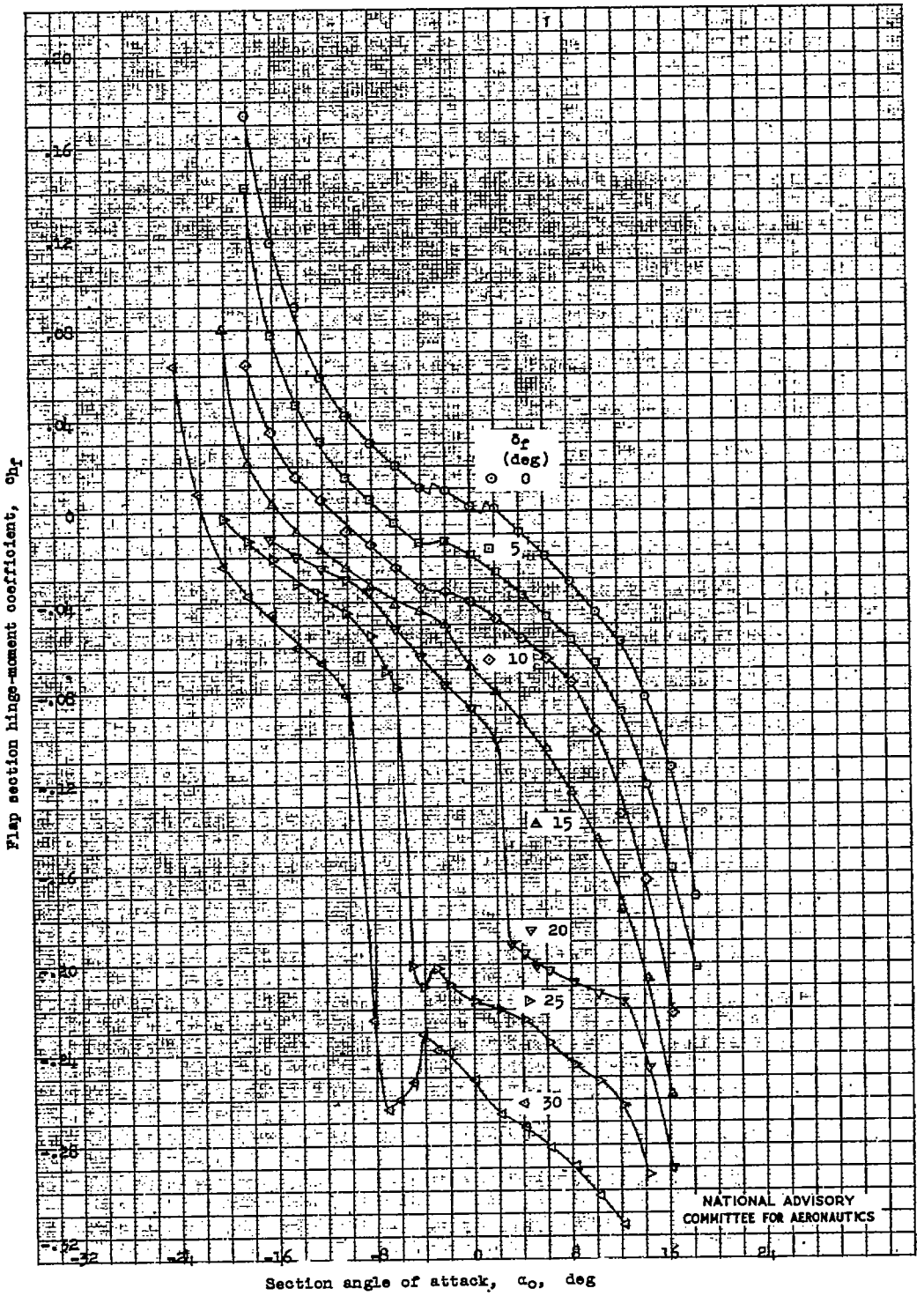

(a) Flap and tab gaps unsealed; $\delta_t = 0°$.

Figure 6.- Hinge-moment characteristics of a 0.40c flap having a 0.333c_f overhang and a 0.20c_f tab on the 10.7-percent-thick symmetrical tail section. $R = 6 \times 10^6$ (approx.); tests, TDT 761 and 765.

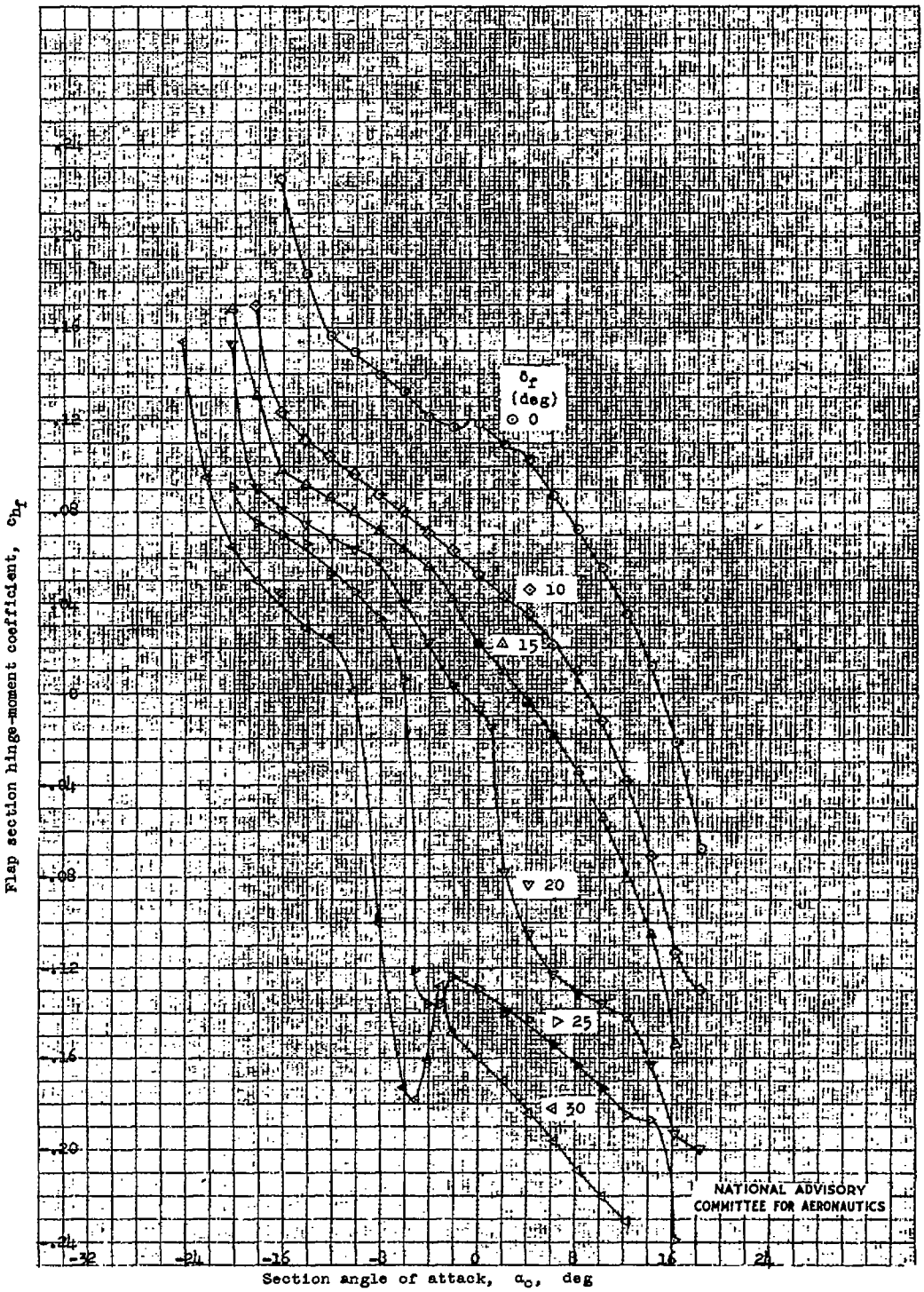

(b) Flap and tab gaps unsealed; $\delta_t = -10°$.

Figure 6 .- Continued.

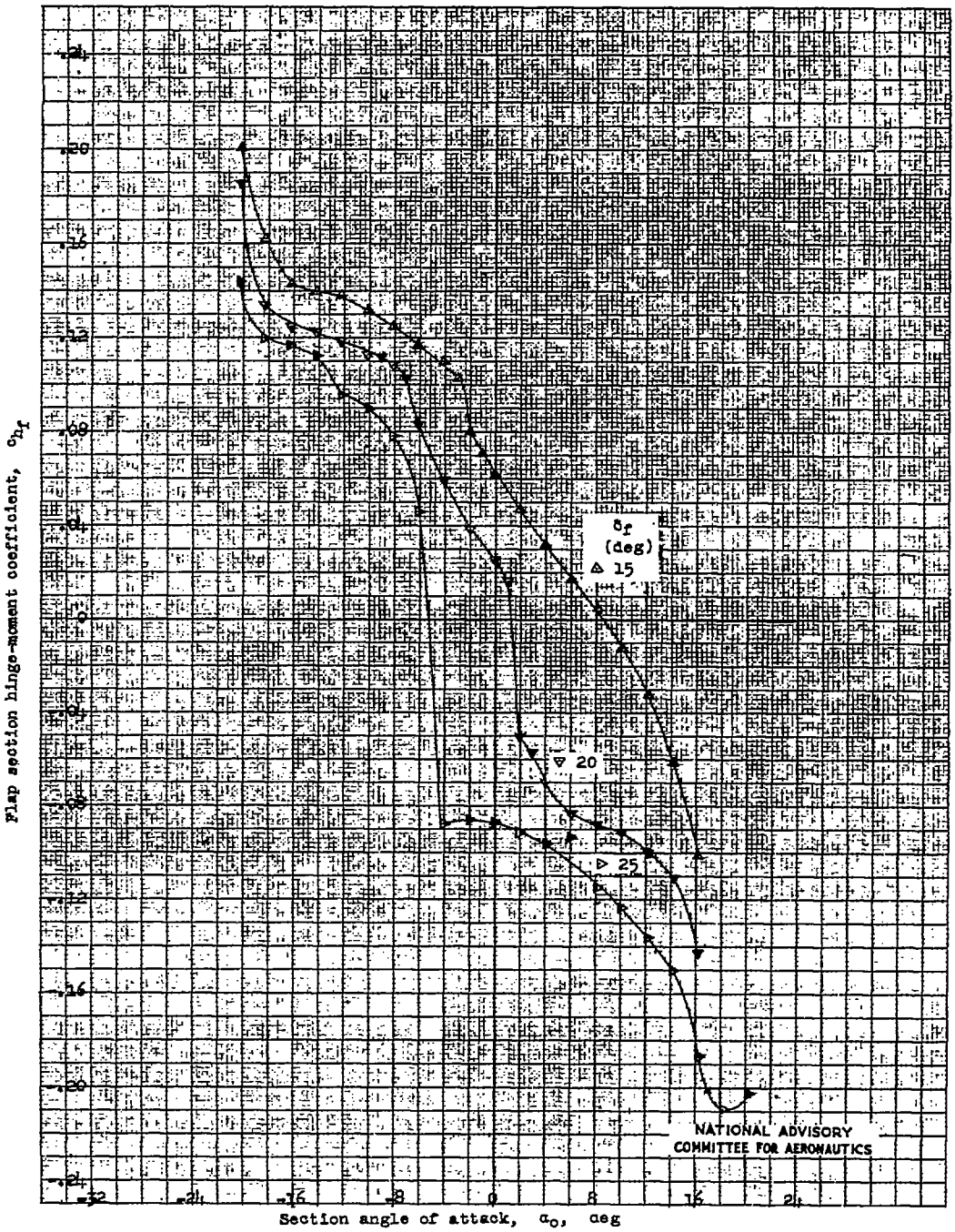

(c) Flap and tab gaps unsealed; $\delta_t = -15^\circ$.

Figure 6 .- Continued.

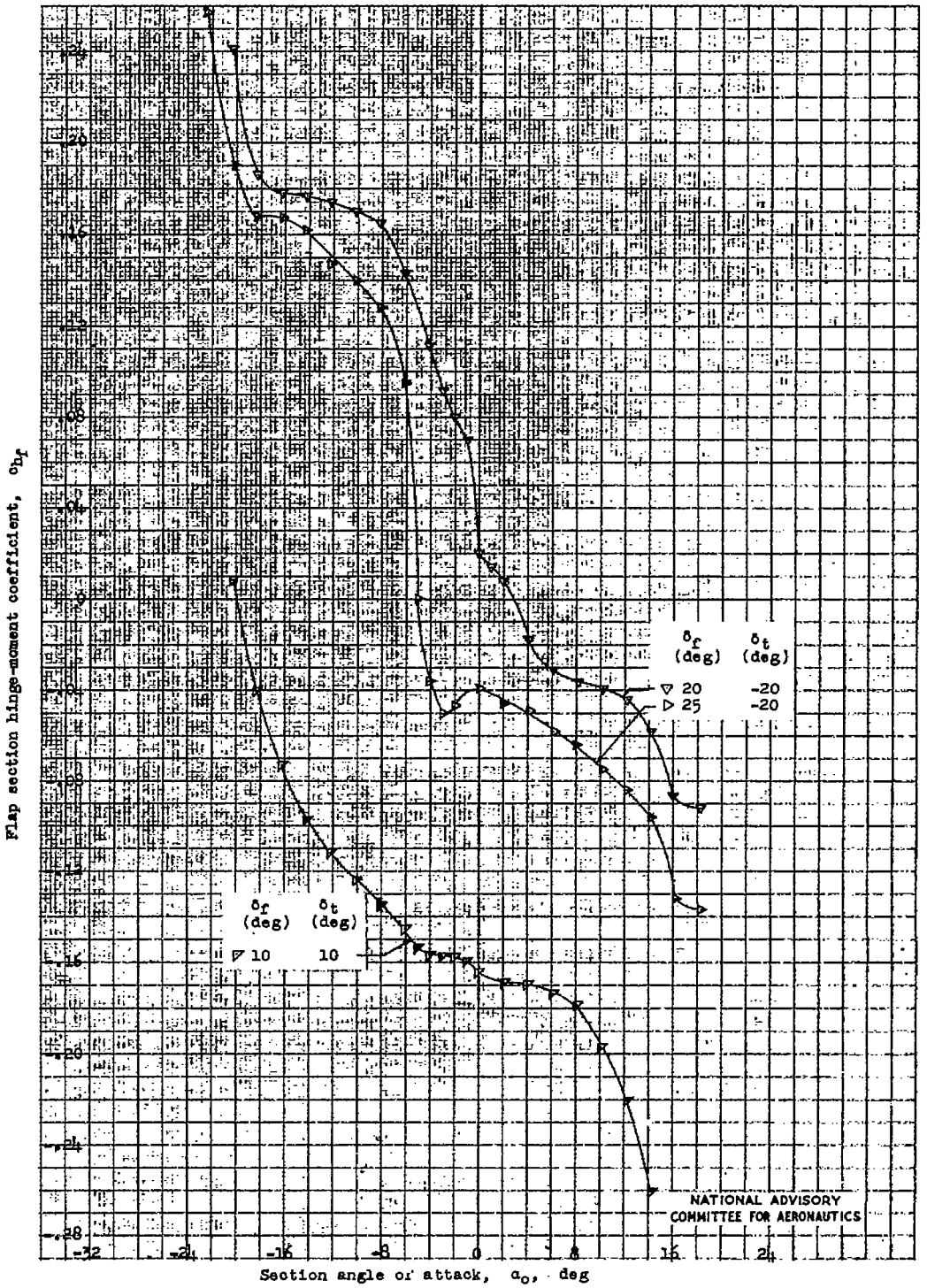

(d) Flap and tab gaps unsealed; $\delta_t = -20^\circ$ and 10°.

Figure 6 .- Continued.

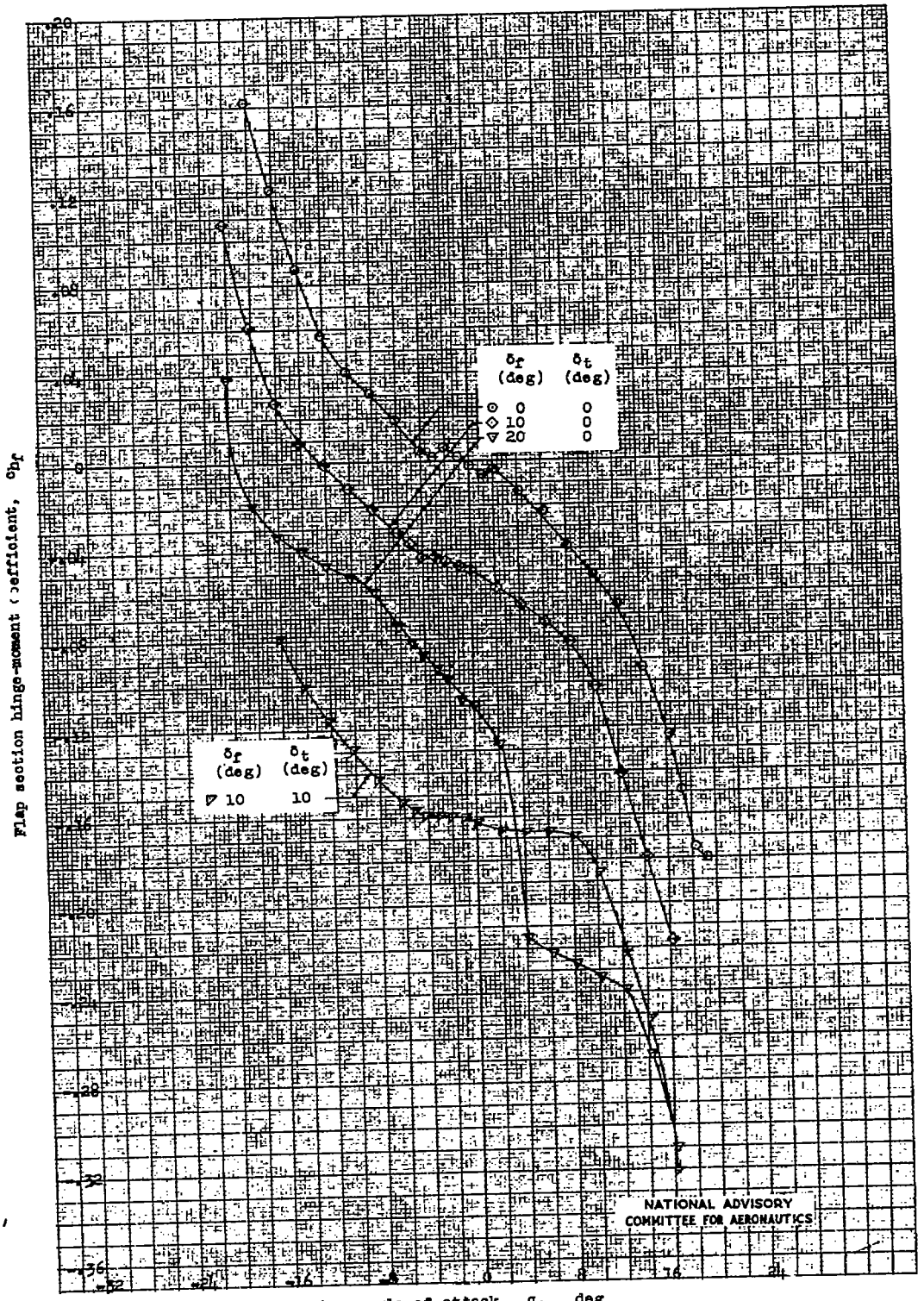

(e) Flap gap unsealed, tab gap sealed; $\delta_t = 0^\circ$ and 10°.

Figure 6 .- Continued.

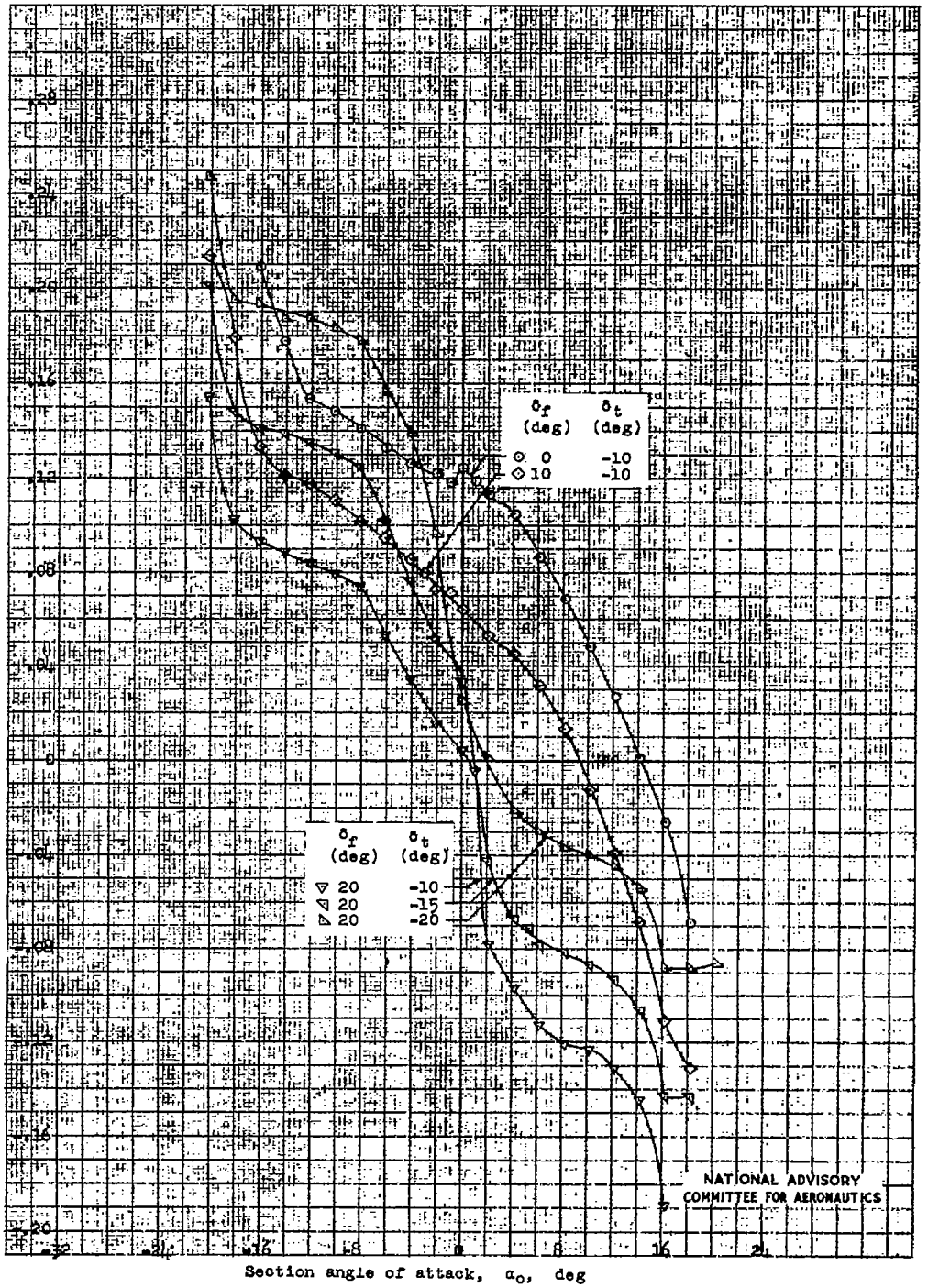

(f) Flap gap unsealed, tab gap sealed; $\delta_t = -10^\circ$, -15°, and -20°.

Figure 6 .- Continued.

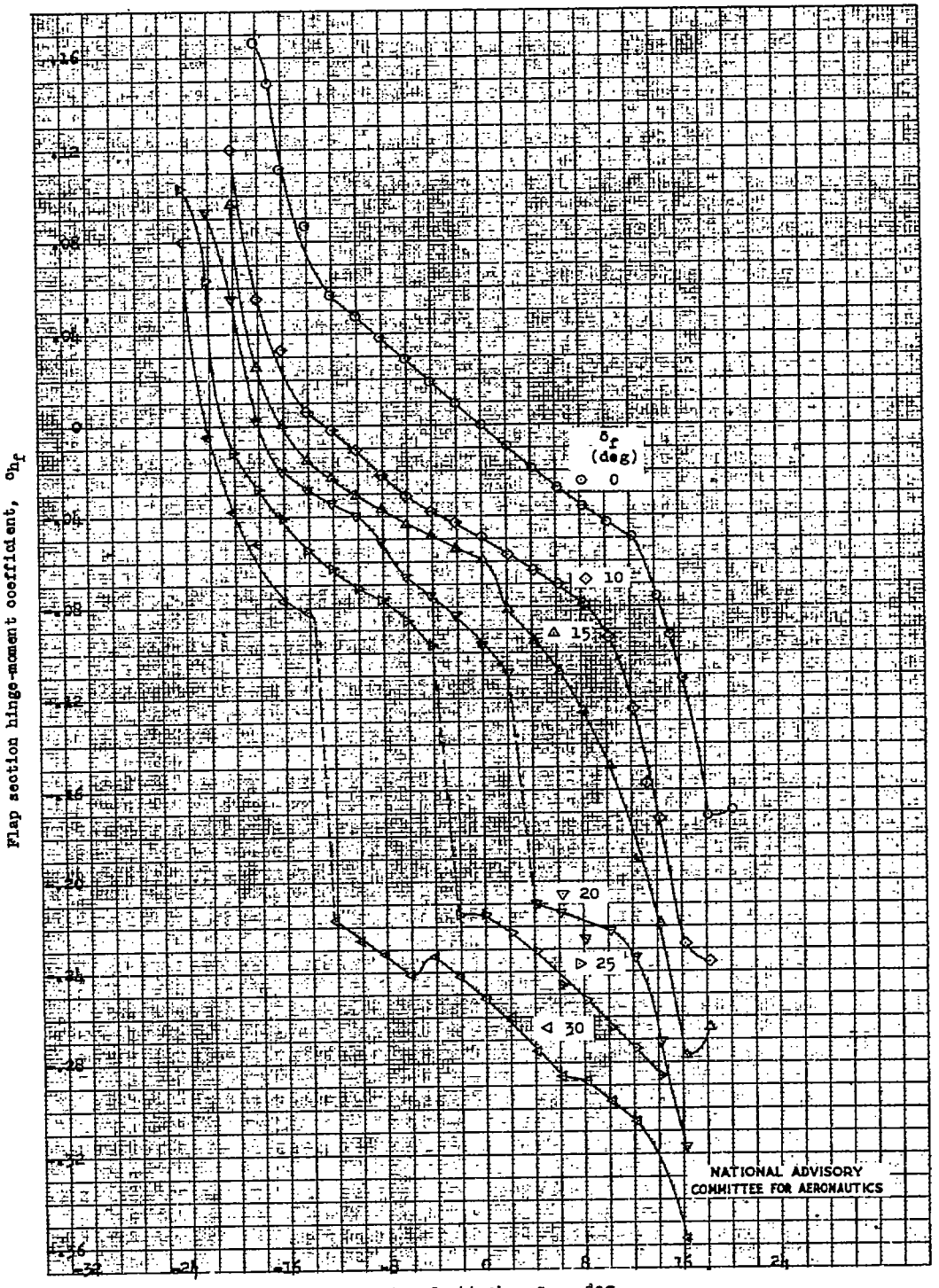

(g) Flap gap sealed, tab gap unsealed; $\delta_t = 0^\circ$.

Figure 6 .- Concluded.

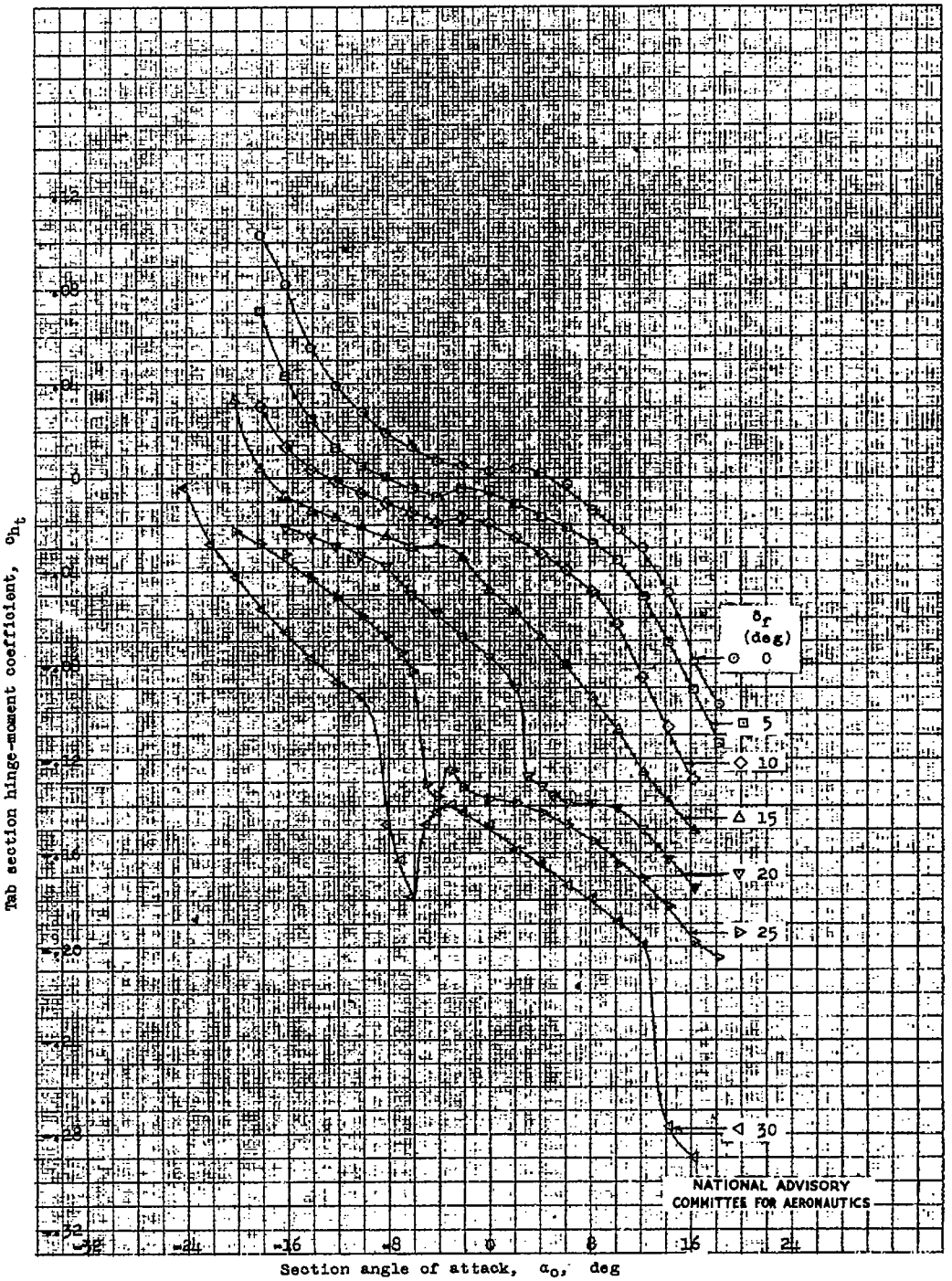

(a) Flap and tab gaps unsealed; $\delta_t = 0^\circ$.

Figure 7.- Hinge-moment characteristics of a $0.20c_f$ tab on a $0.40c$ flap having a $0.333c_f$ overhang on the 10.7-percent-thick symmetrical tail section. $R = 6 \times 10^6$ (approx.); tests, TDT 761 and 765.

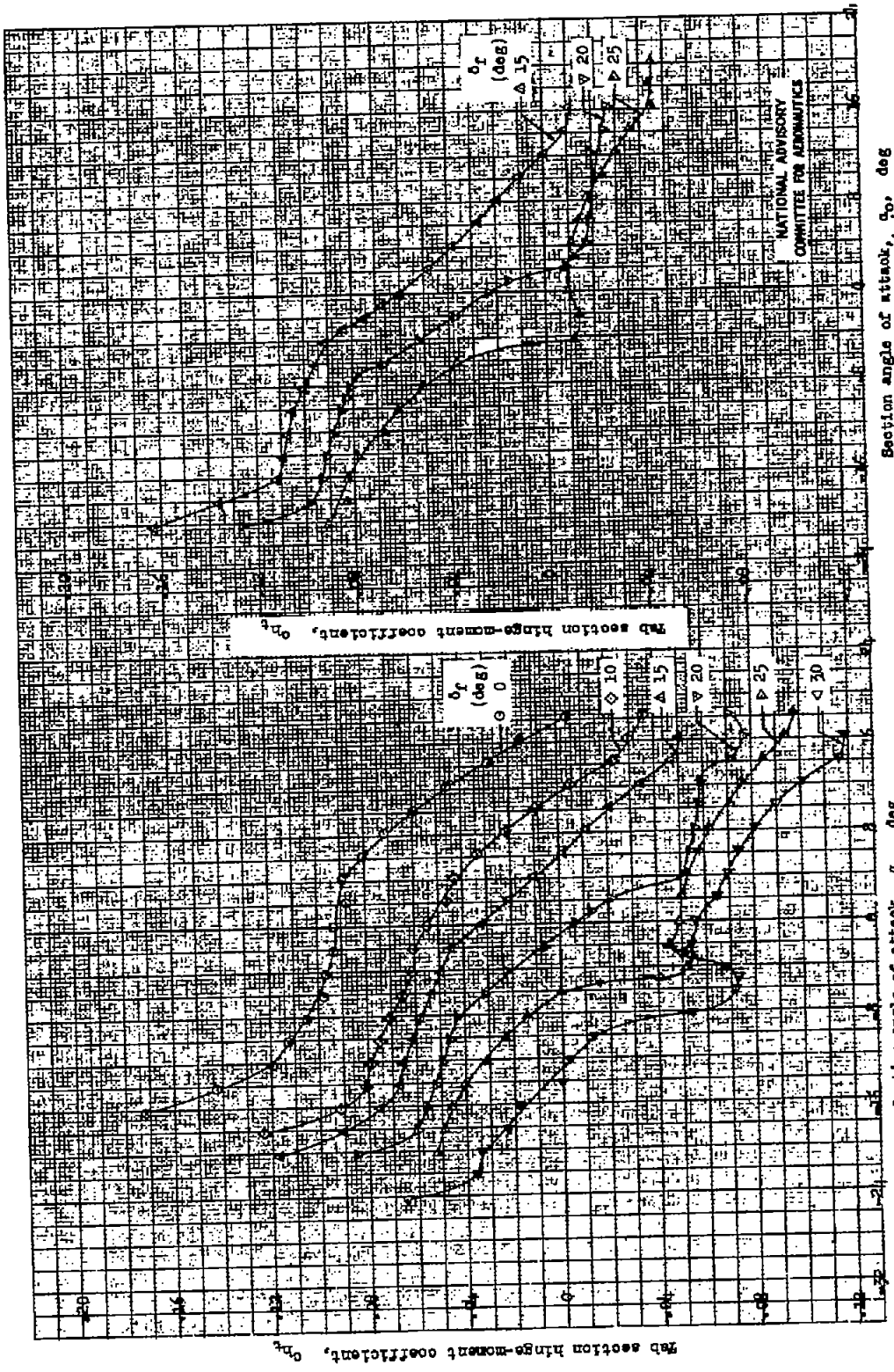

(b) Flap and tab gaps sealed; $\delta_t = -10°$.

(c) Flap and tab gaps unsealed; $\delta_t = -15°$.

Figure 7.- Continued.

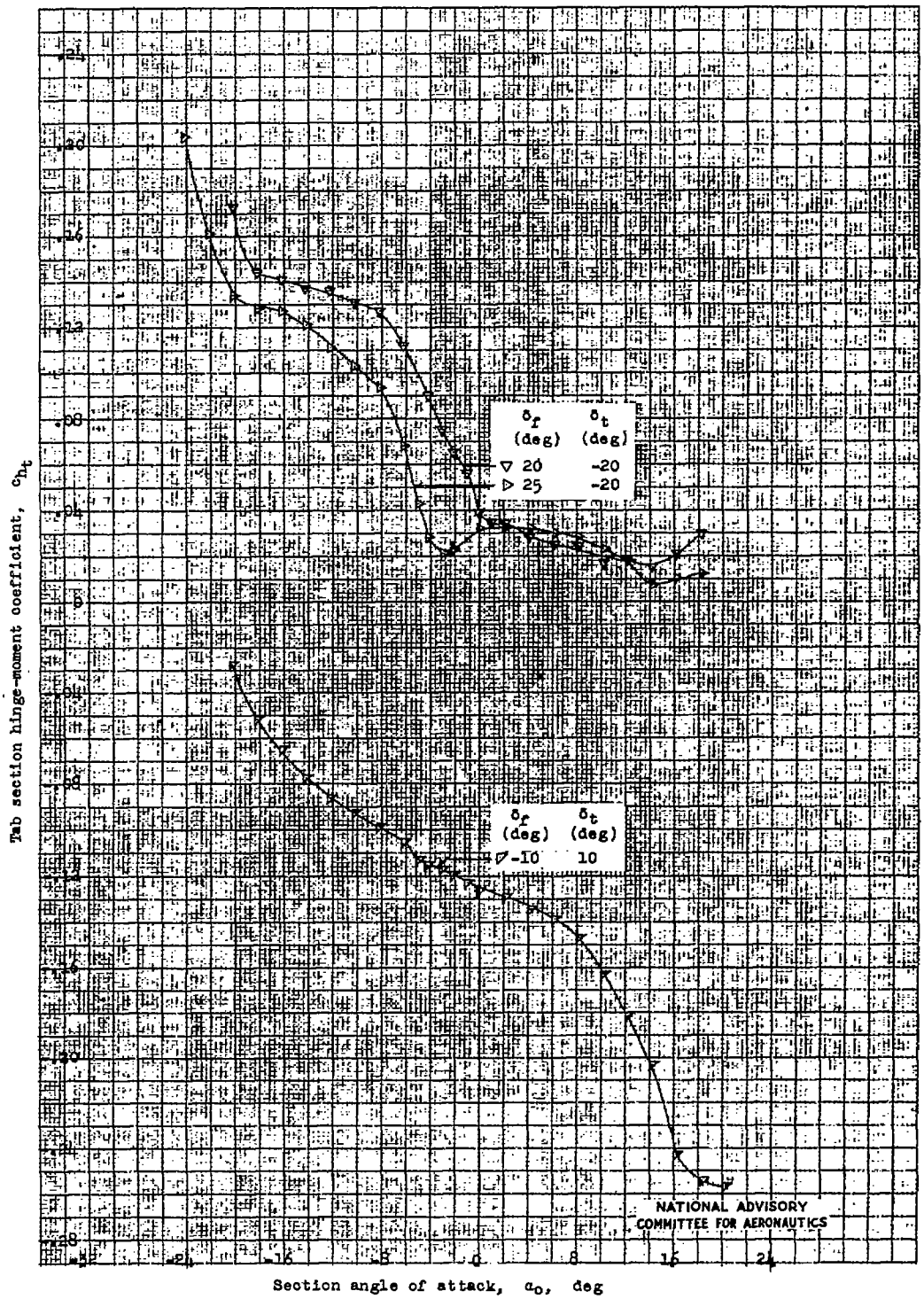

(d) Flap and tab gaps unsealed; $\delta_t = -20^\circ$ and 10°.

Figure 7 .- Continued.

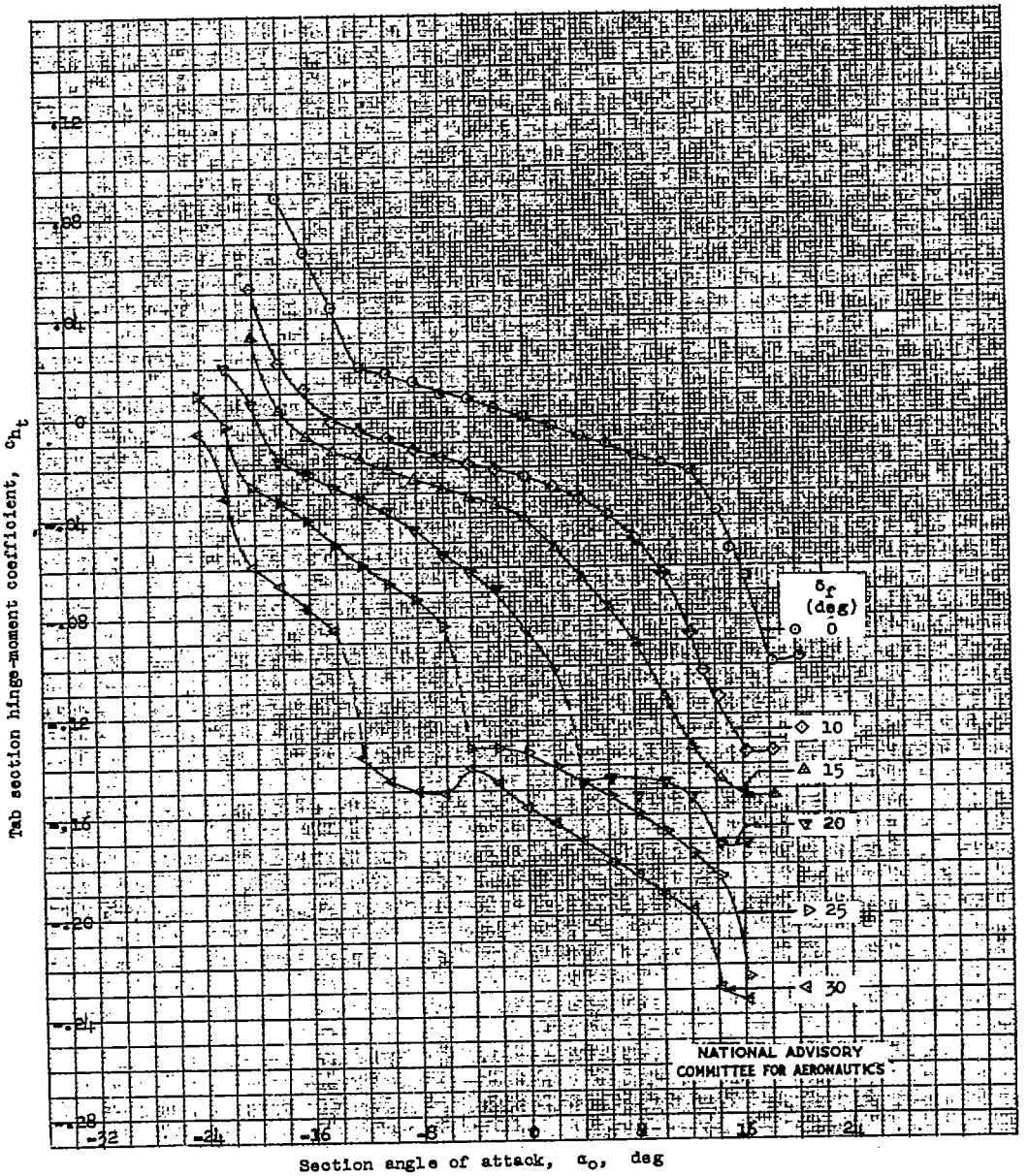

(e) Flap gap sealed, tab gap unsealed; $\delta_t = 0^\circ$.

Figure 7 .- Concluded.

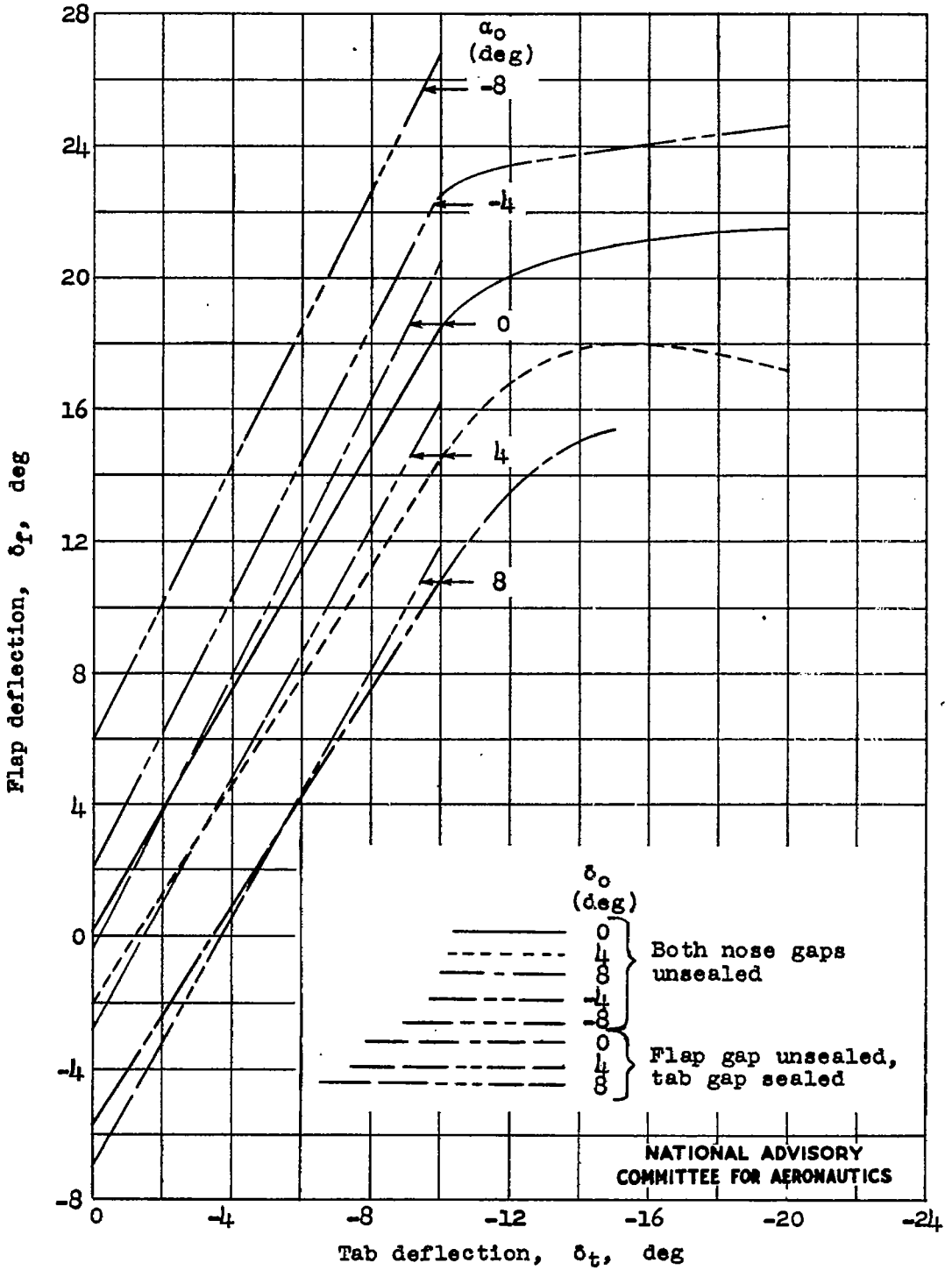

Figure 8.- Variation of flap deflection with the tab deflection required to maintain a constant flap section hinge-moment coefficient of 0. $R = 6 \times 10^6$ (approx.).

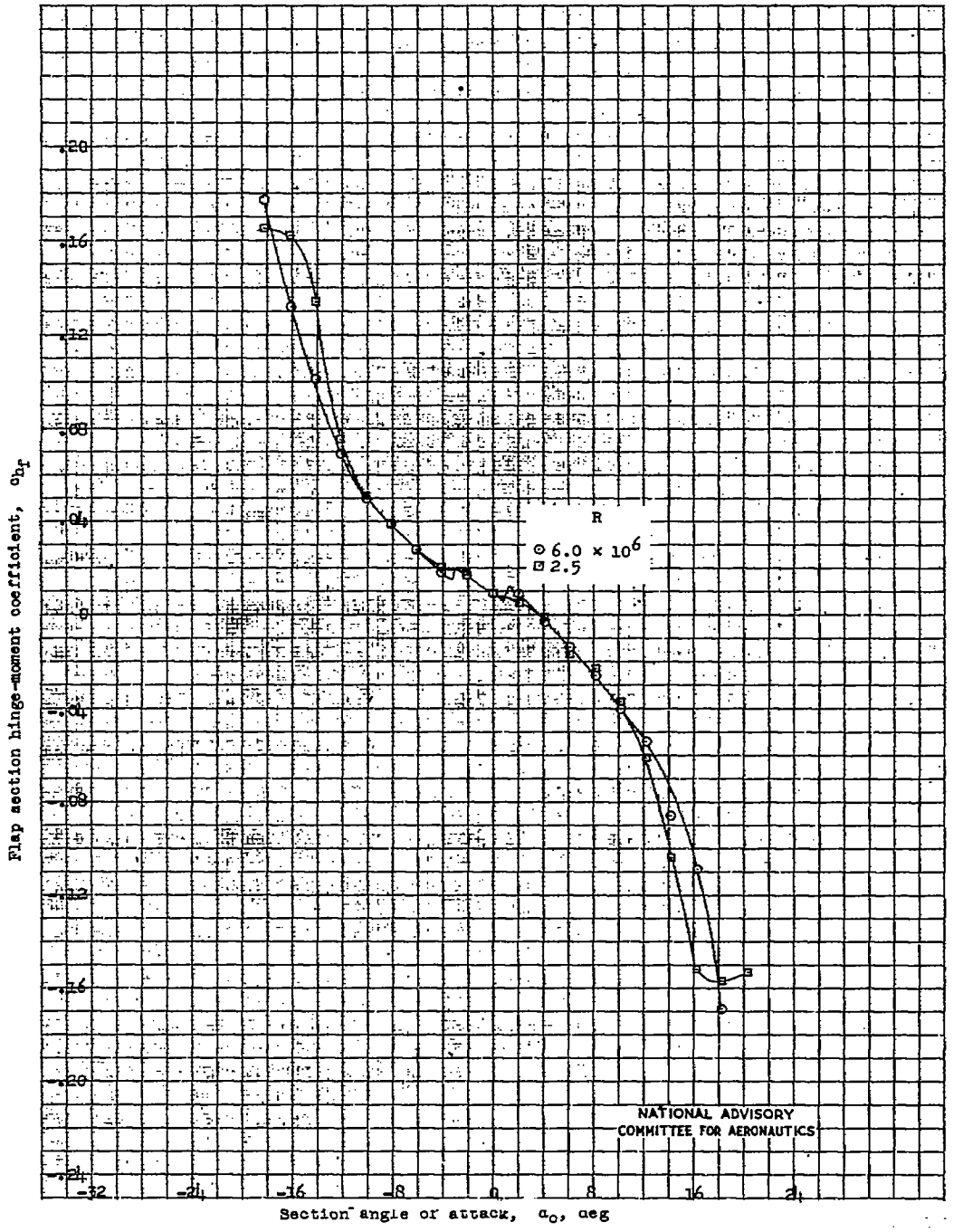

(a) Flap hinge-moment characteristics.

Figure 9.- Scale effect on hinge-moment characteristics of a 0.40c flap and a 0.20c_f tab on the 10.7-percent-thick symmetrical tail section. Flap and tab gaps unsealed; $\delta_f = 0°$, $\delta_t = 0°$; test, TDT 761.

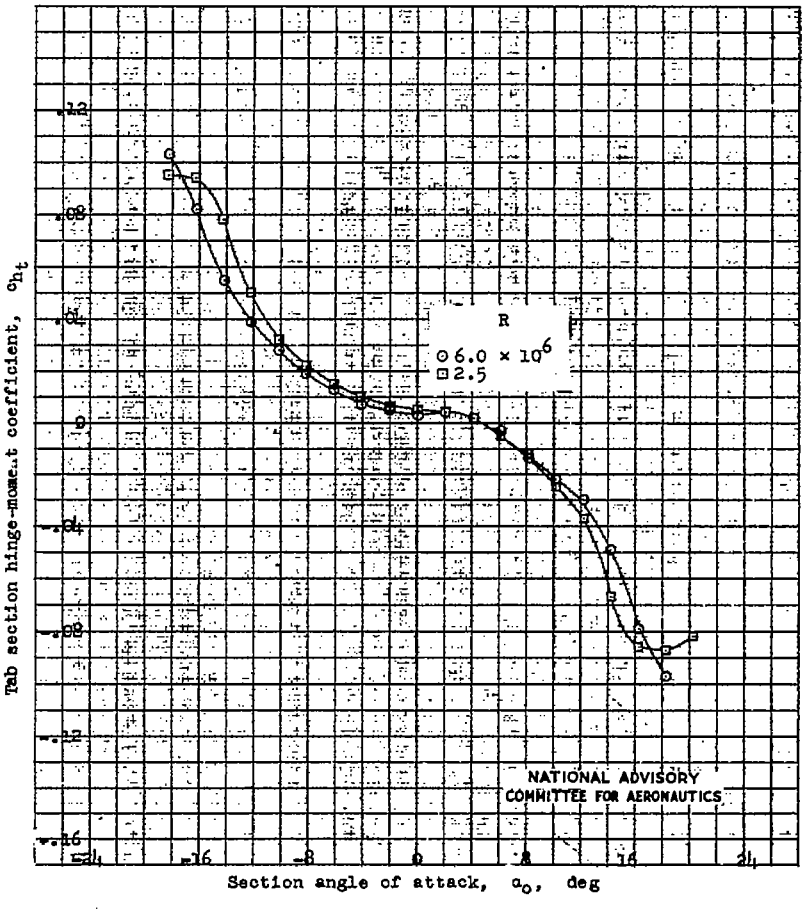

(b) Tab hinge-moment characteristics.

Figure 9 .- Concluded.

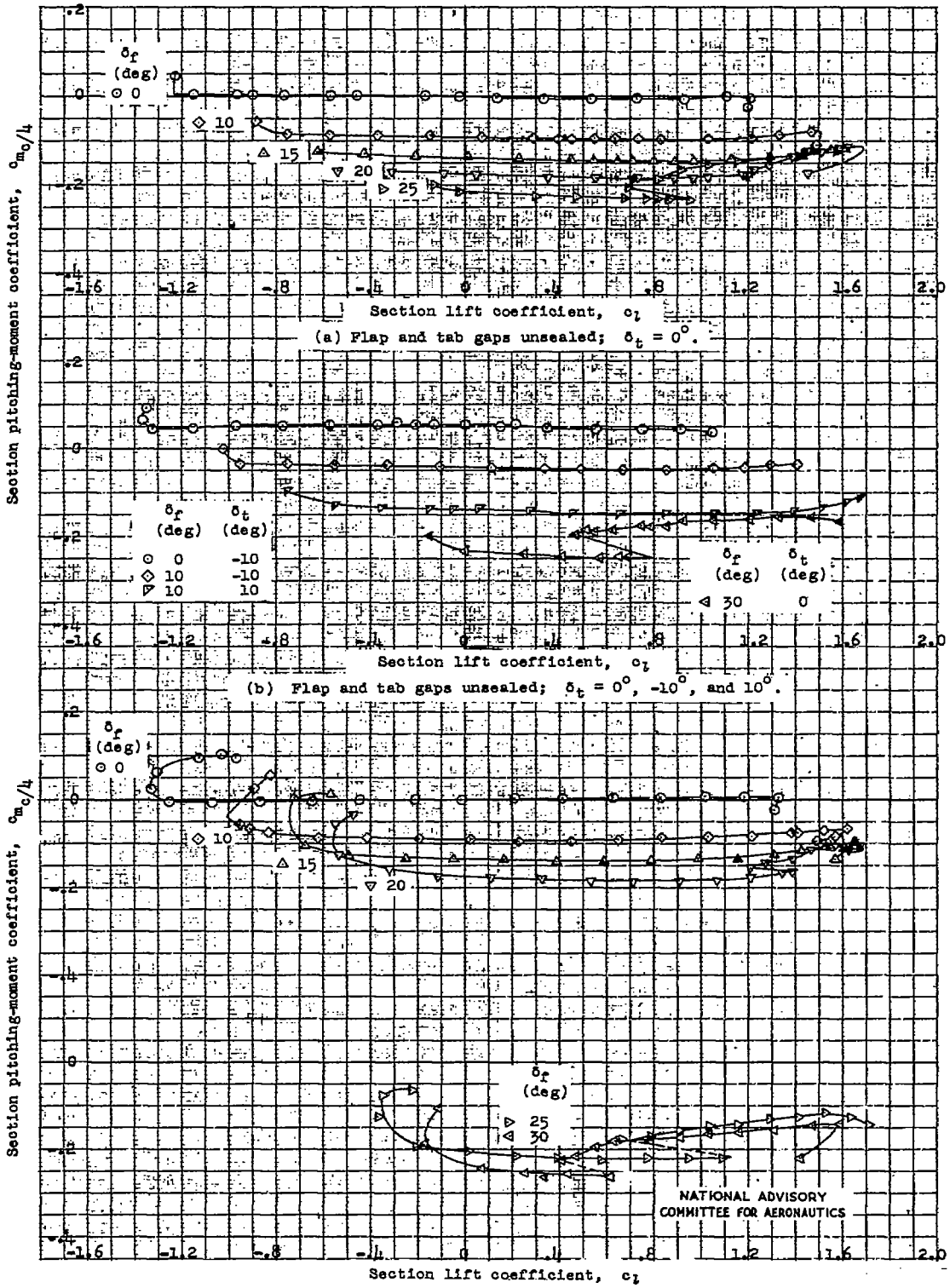

(a) Flap and tab gaps unsealed; $\delta_t = 0^\circ$.

(b) Flap and tab gaps unsealed; $\delta_t = 0^\circ$, -10°, and 10°.

(c) Flap gap sealed, tab gap unsealed; $\delta_t = 0^\circ$.

Figure 10.- Pitching-moment characteristics of the 10.7-percent-thick symmetrical tail section with a 0.40c flap having a 0.333c_f overhang and a 0.20c_f tab. $R = 6 \times 10^6$ (approx.); tests, TDT 753 and 764.

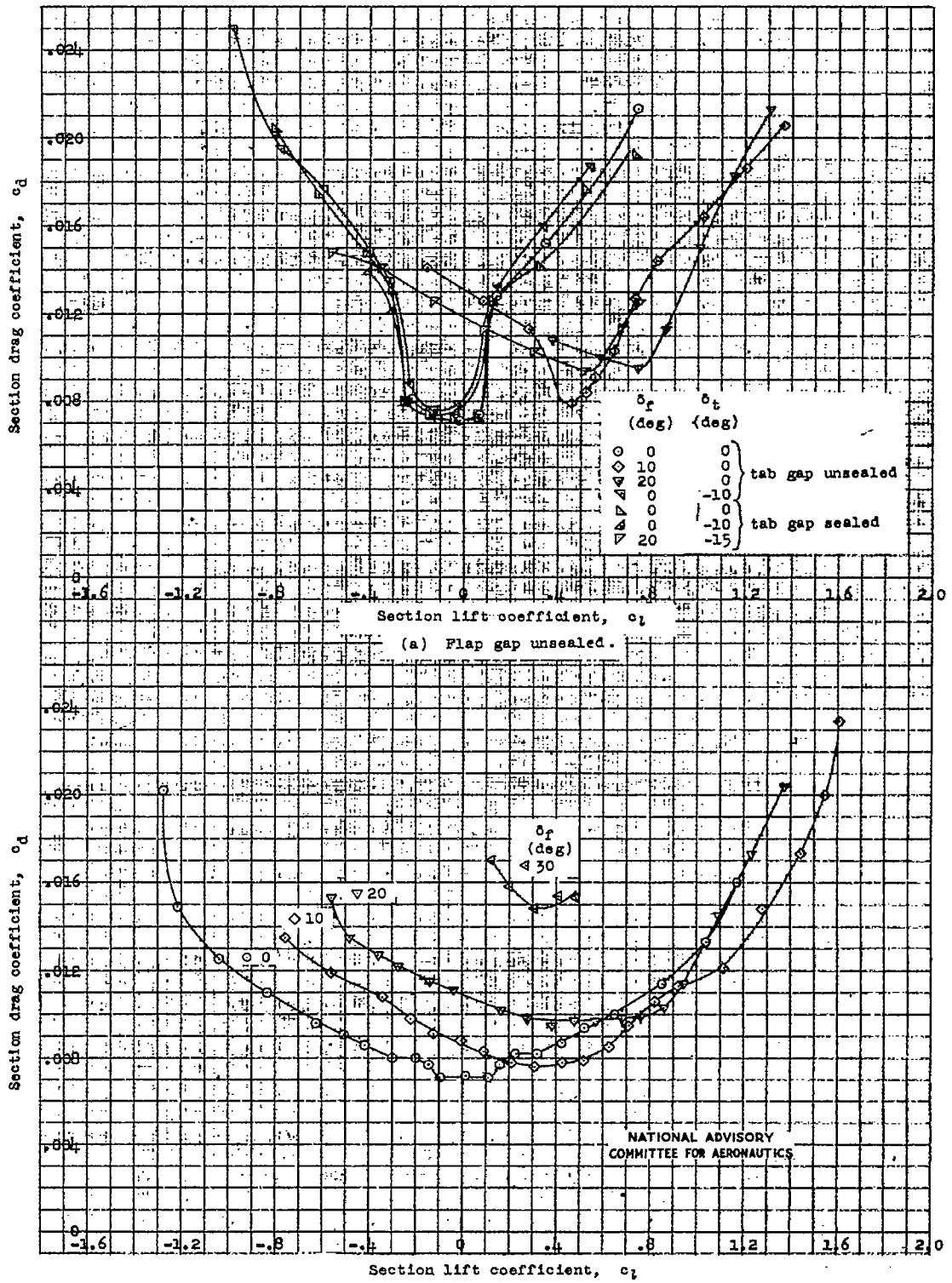

Figure 11.- Drag characteristics of the 10.7-percent-thick symmetrical tail section with a 0.40c flap having a 0.333c_f overhang and a 0.20c_f tab. $R = 6 \times 10^6$ (approx.); tests, TDT 753, 755, and 765.